Plasmonic 2D and 3D Microstructures: Assembly and Applications

Dr. Alexey Yashchenok

Max-Planck Institute of Colloids and Interfaces, Potsdam, Germany

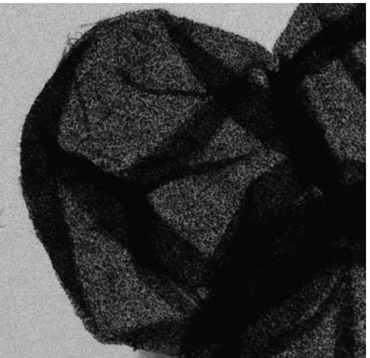

50th Zakopane School of Physics, 18-23 May 2015

Colorful motifs of plasmonic

Windows in Churches

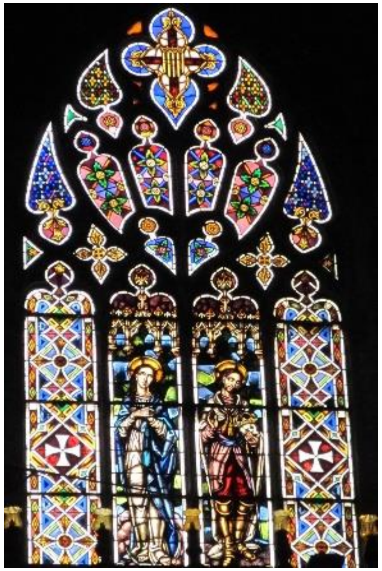

LYCURGUS CUP,
Roman goblet dating from the fourth century A.D.

Light out

Light in

Origin of plasmonic

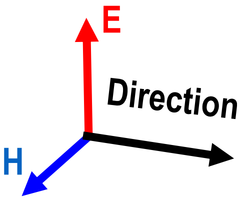

Induced dipole

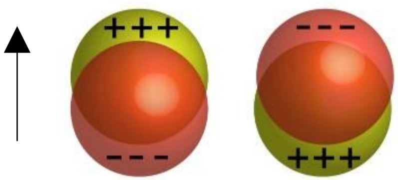

$$p \propto \left(\frac{\varepsilon(\lambda) - \varepsilon_m}{\varepsilon(\lambda) + 2\varepsilon_m} \right)$$

$$\sigma_{abs} = 4\pi k r^3 Im \left| \frac{\varepsilon_p - \varepsilon_m}{\varepsilon_p + 2\varepsilon_m} \right|^2$$

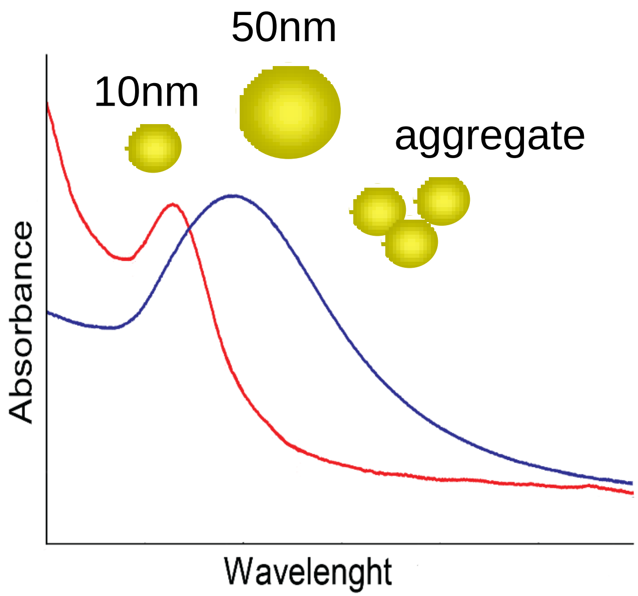

$$\varepsilon_p = 1 - \frac{\omega_p^2}{\omega^2}$$

Refractive index

1.336 ⟶ 1.583

Plasmonic Structures

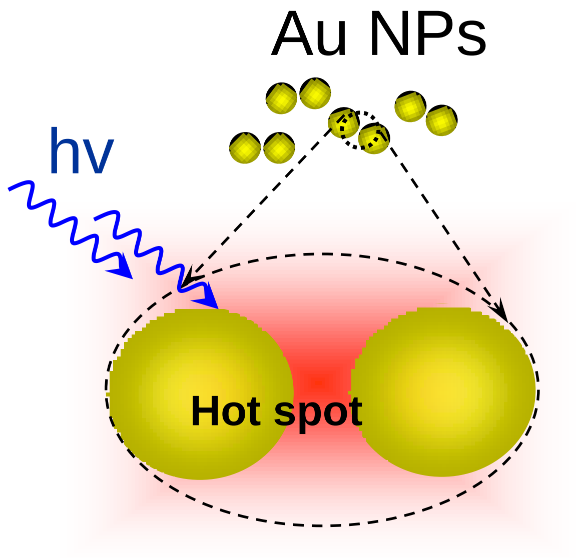

Rayleigh scattering
Photoluminescence
Raman scattering
Heating
Photoacoustic

Bio-Sensing
Molecules Release
Cancer treatment
Cell manipulation
Advanced coatings
Optoelectronics

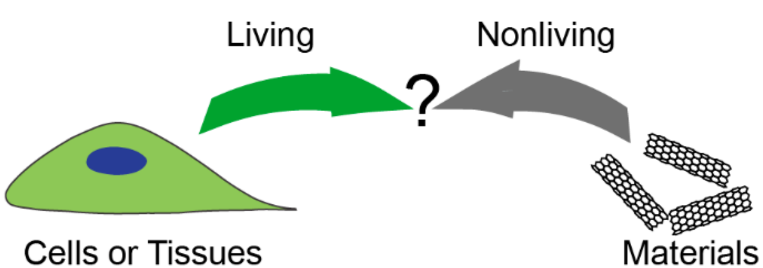

Raman spectroscopy

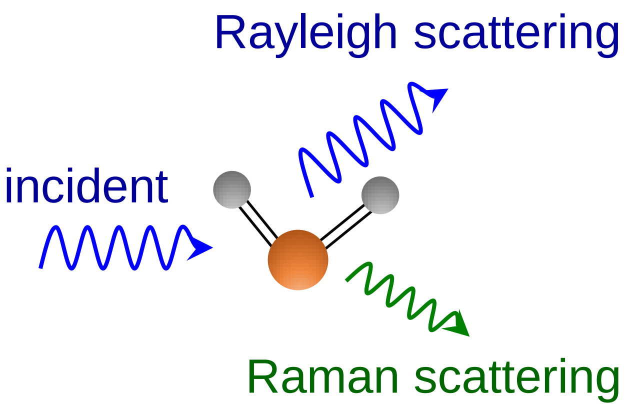

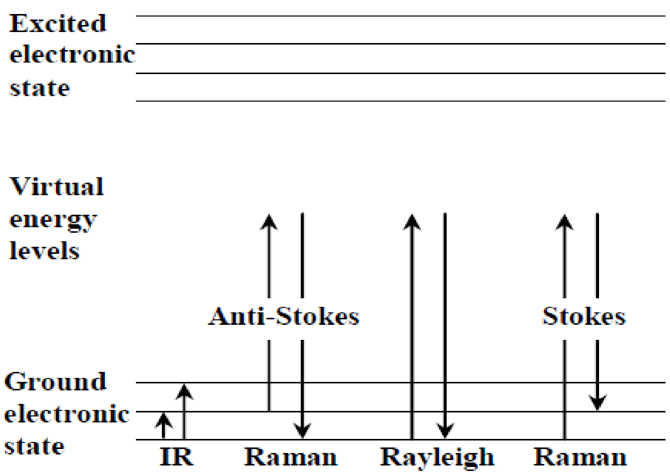

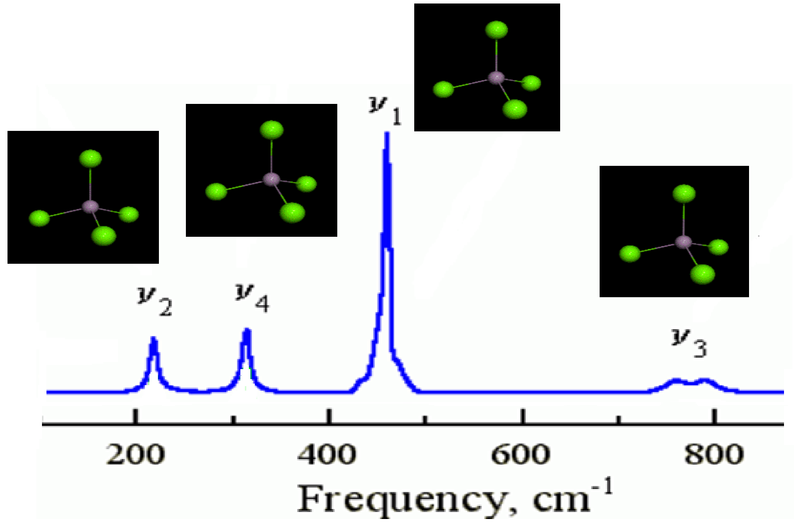

Non-invasive
Fingerprint of molecules
Label-free

Diagnostics, Pharmacy, Art

Cross section = σ_R 10^{-31}-10^{-29} cm^2/mol

http://fy.chalmers.se/OLDUSERS/brodin/MolecularMotions/CCl4molecule.html

Surface enhanced Raman scattering (SERS)

$$h\nu = h\nu_R + h\nu'$$

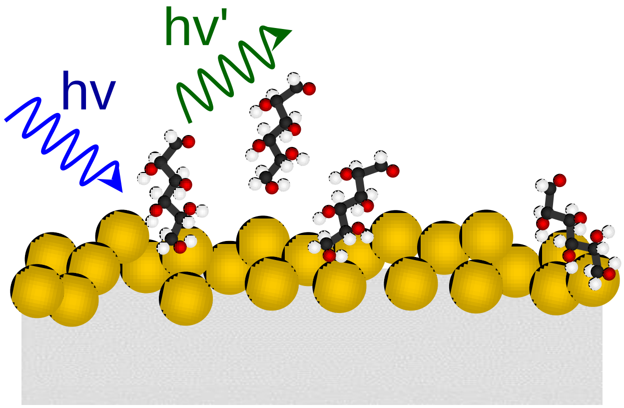

Roughened metal surface
Enhancement 10^{6-8}

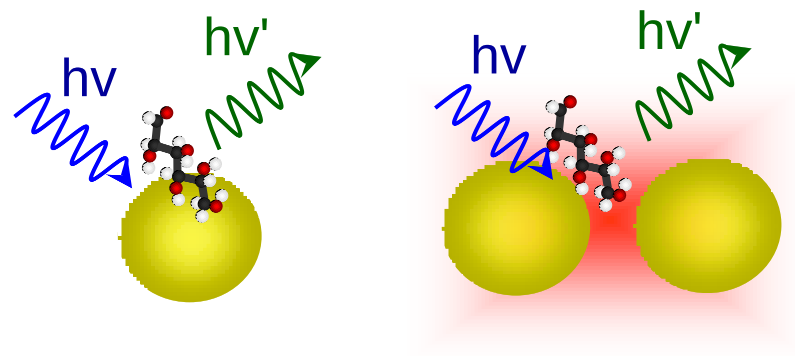

Single particles or Aggregates
Enhancement 10^{8-15}

Acquiring signal from tiny volume

Cross section ≈ 10^{-16} cm^2/mol

Nie, Emory, Science, 275, 1102, 1997; Kneipp, et al. PRL, 78, 1667, 1997

Mechanism of SERS

$$P^{RS}(\nu_s) = N\sigma^{R}_{free} I(\upsilon_L)$$

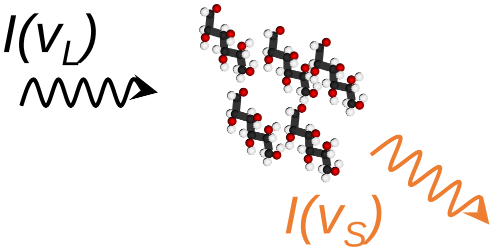

Local Field Enhancement

- Enhancement of the local excitation field
- Enhancement of the local Raman scattering field

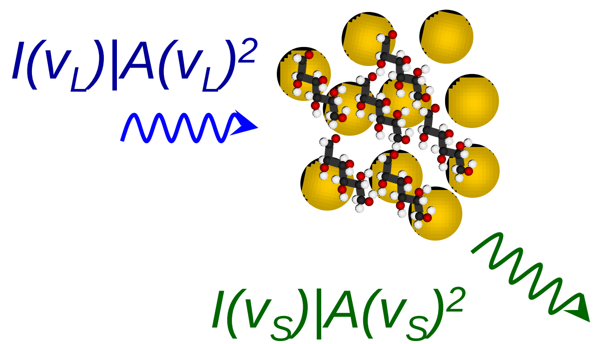

$$P^{SERS}(\nu_s) = N\sigma^{R}_{ads} |A(\upsilon_L)|^2 |A(\upsilon_s)|^2 I(\upsilon_L)$$

Increase of the Raman scattering cross section

- Electronic coupling between molecule and metal (chemical effect)

Amplification of lipids and glycocalix by Au-NPs

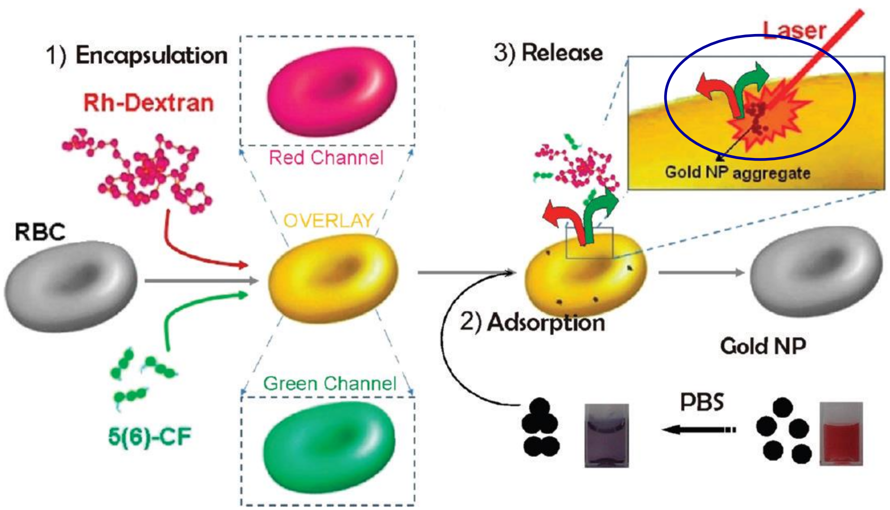

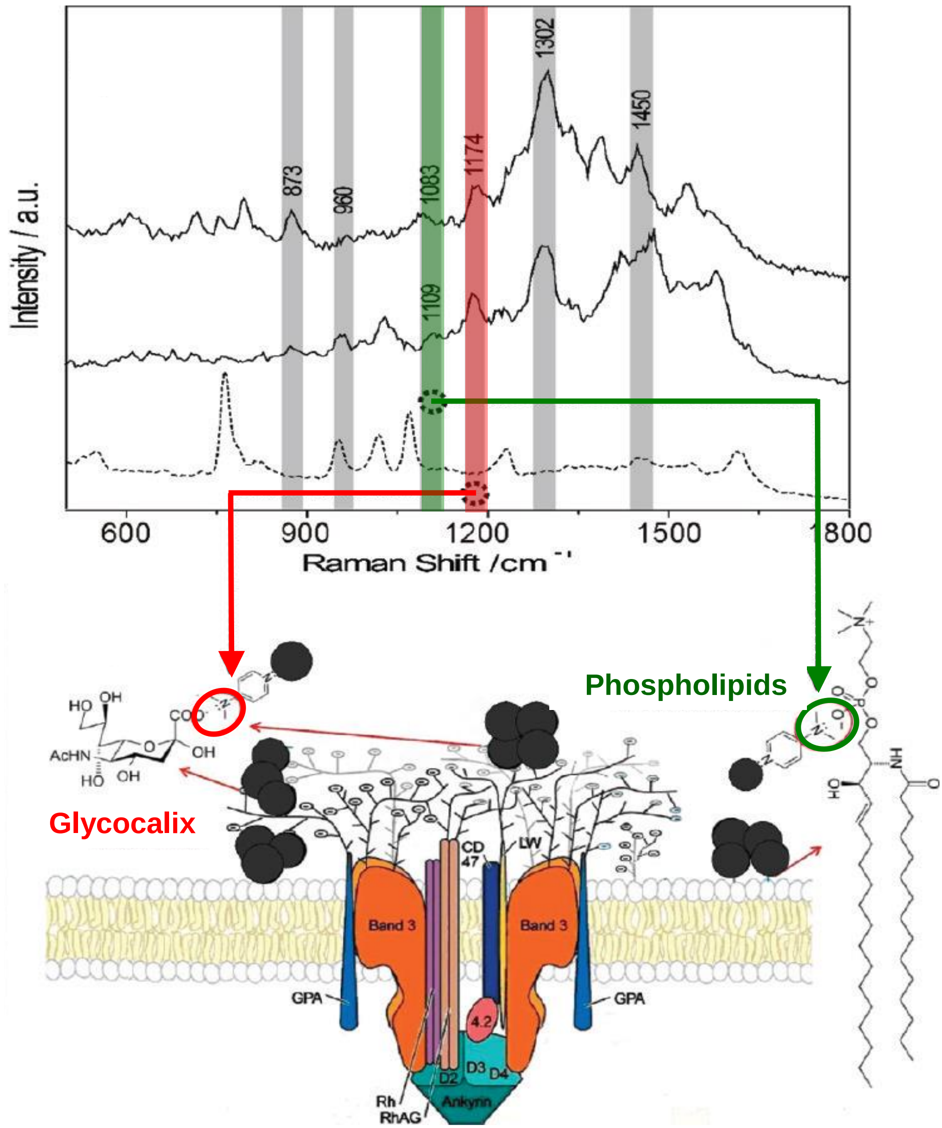

M. Delcea, N. Sternberg, A.M. Yashchenok et al. ACSNano, 2012, 6, 4169.

Controlled assembly of plasmonic nanoparticles

<u>Top-down</u>

nanosphere lithography; etching; vacuum deposition

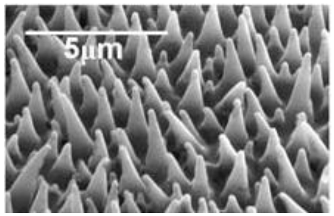

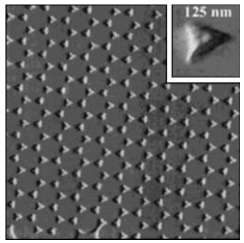

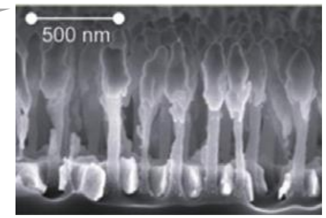

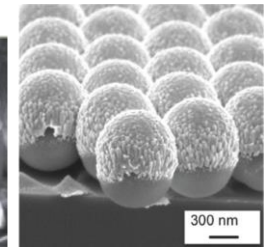

Plasmonic substrates

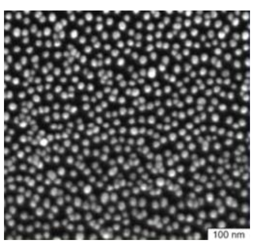

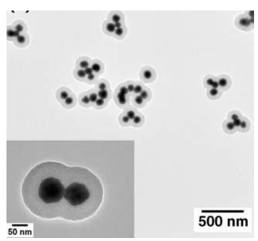

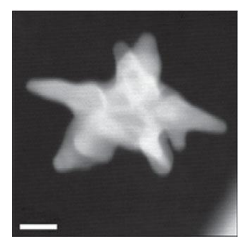
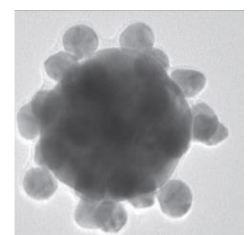

<u>Bottom-up</u>

drop casting; spin coating; chemical growth; nanolitoghraphy;
self-assembly; Langmuir-Blodgett; Layer-by-Layer

J. R. Soc. Interface (2010) 7, S435. Anal. Bioanal. Chem. (2009), 394, 1819. Acc. Chem. Res. 2006, 39, 443.; Small 2011, 7, No. 24, 3445.

Self-assembly technique

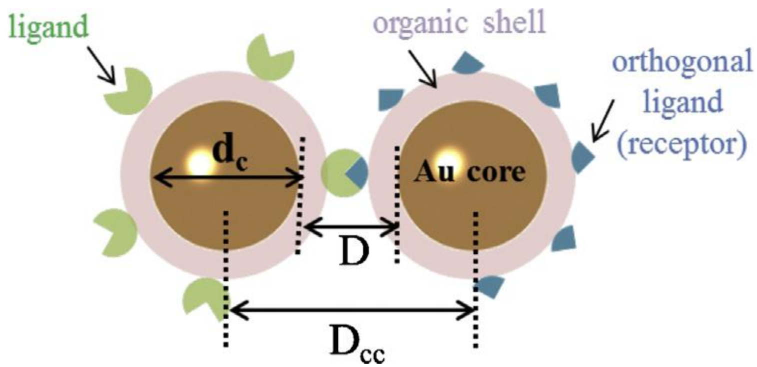

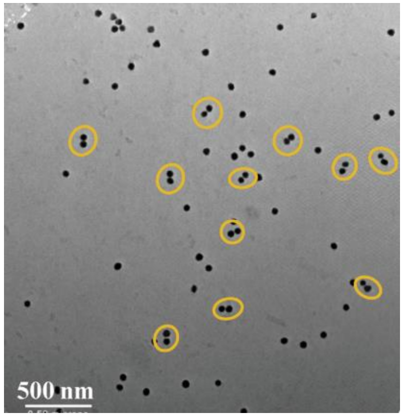

Nano Today (2013) 8, 480.

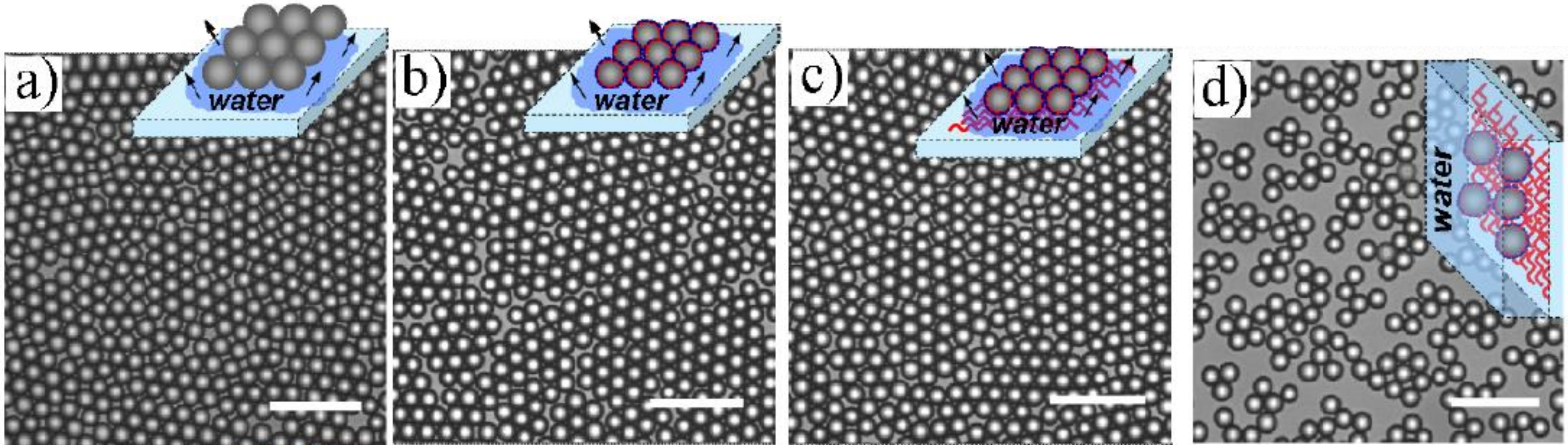

Polymers 2010, 2, 690.

Template-assisted technique

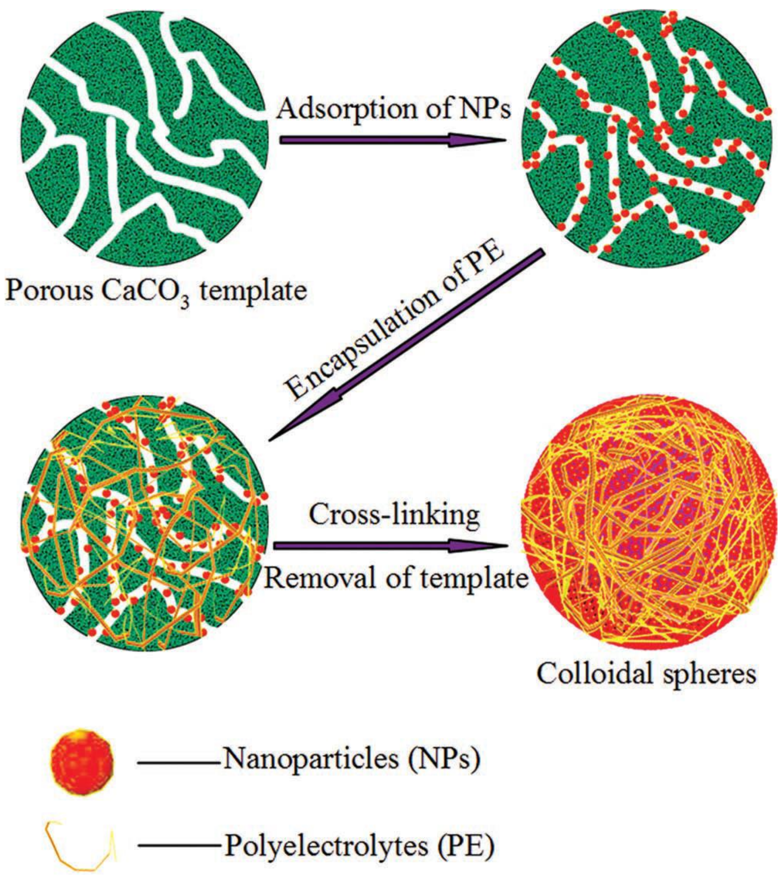

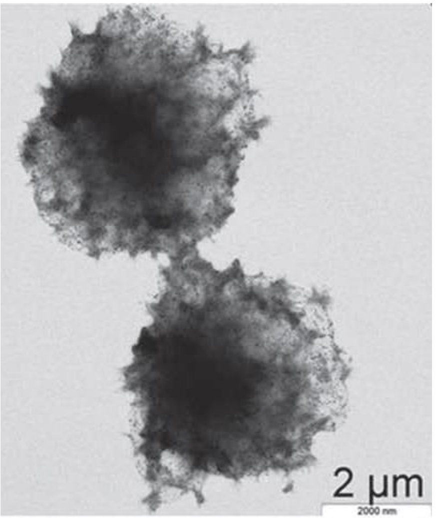

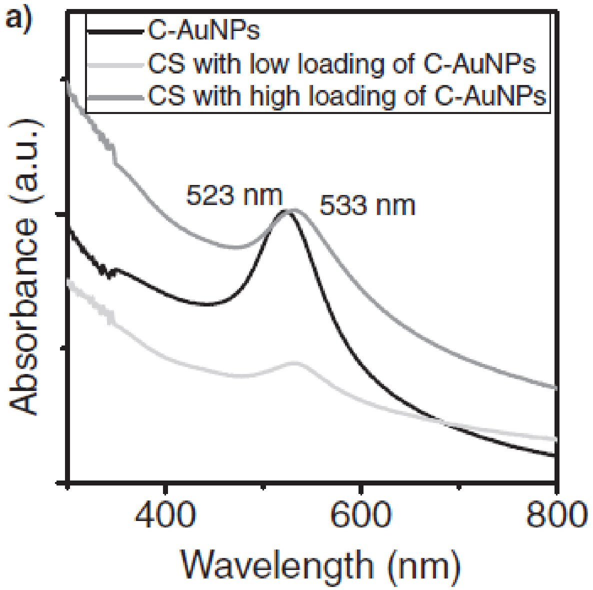

Adv. Mater. **2012**, 24, 2663.

Layer-by-Layer assembly (LbL)

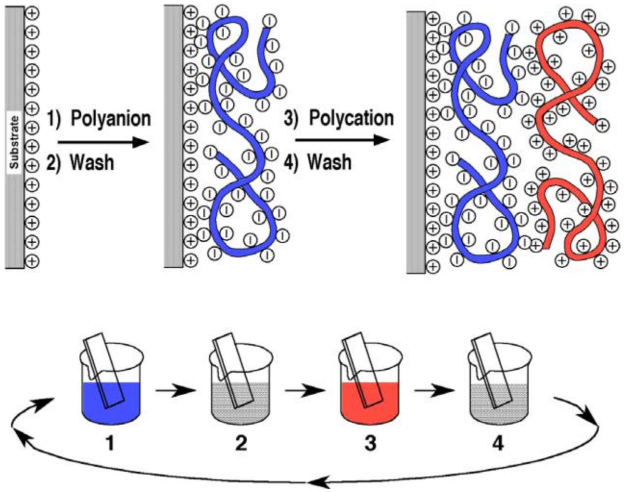

G. Decher, J.D. Hong, Macromol. Chem. Sym., 1991, 46, 321

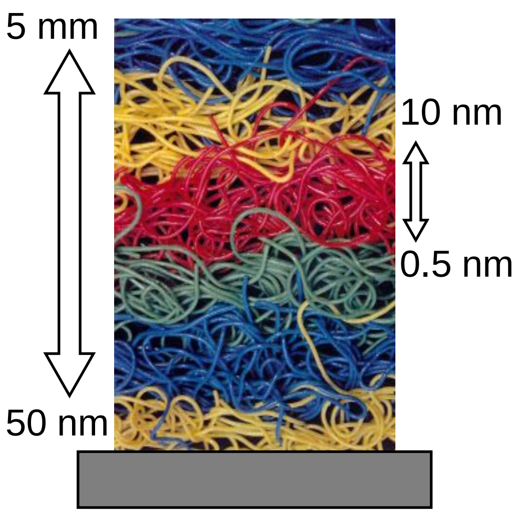

- Can be made on ANY surface
- Control of composition
- Different functionalities
- Materials: polymers, proteins,
- nanoparticles, …
- Components can be fixed or
- mobile
- Porosity control, …

<u>A "real world" Application</u>

Metal Rubber™ (NanoSonic Inc.)

Popular Science, August 2004, page 36

Contact Lenses

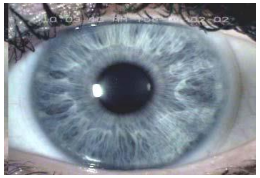

US Patent US 520 8111

LbL hollow multilayer capsules

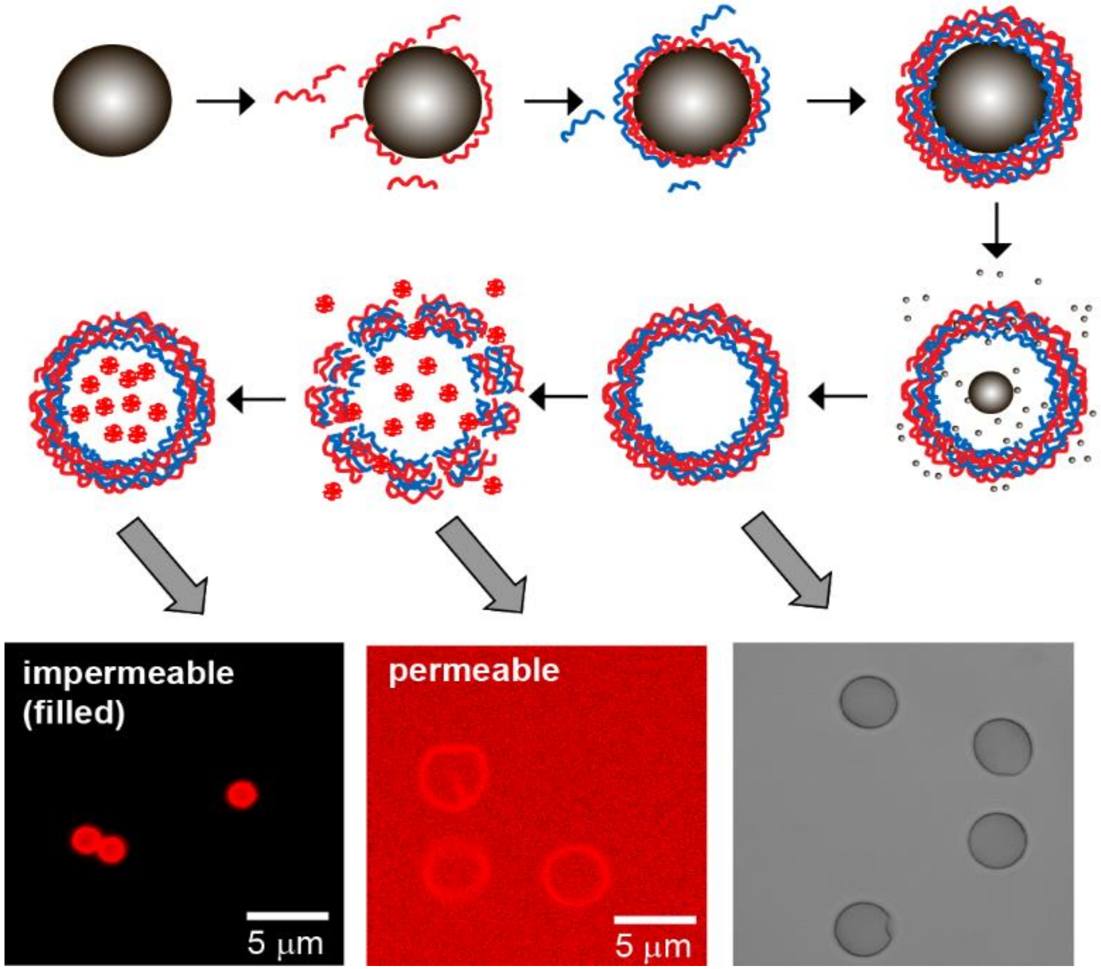

- Shell permeability control
- Loading of molecules > 1kDa
- Colloids from 50 nm to few microns
- Even cells and RBCs can be used

G. B. Sukhorukov, E. Donath, S. Davis, H. Lichtenfeld, F. Caruso, V. I. Popov, H. Möhwald, Polym. Adv. Technol., 1998, 9, 759.

Multilayer shell properties

830 nm

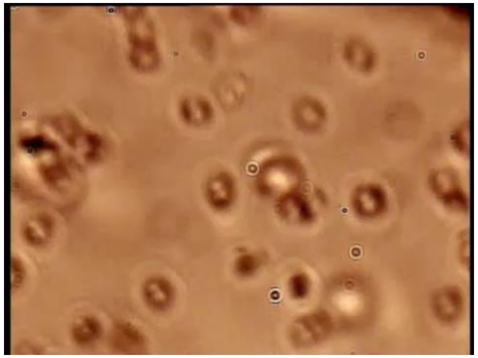

473 nm

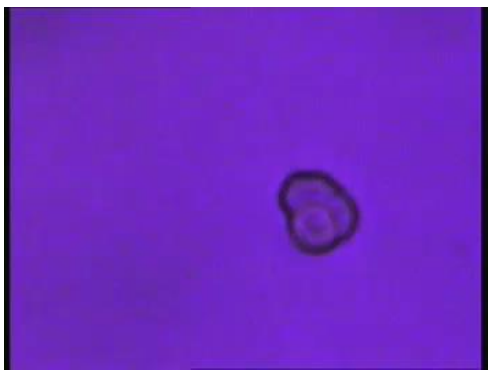

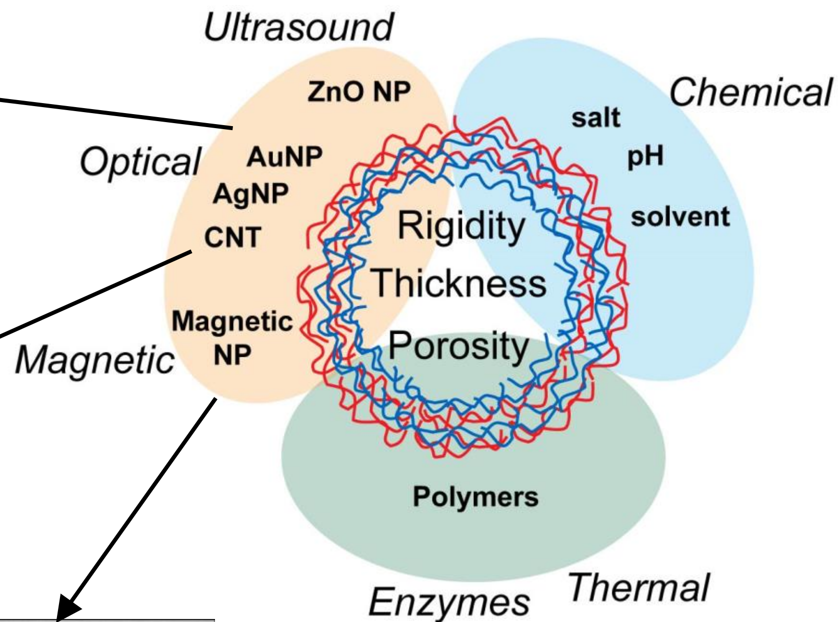

Adv. Funct. Mater. 2010, 20, 3136

PCCP, 2008, 10, 6899

Our Focuses

SERS sensors base on microparticles and microcapsules

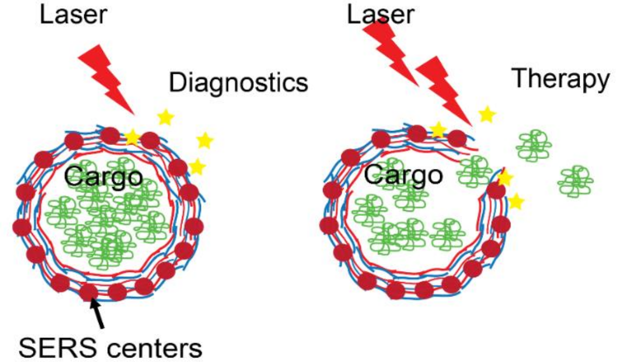

SERS flexible substrates for express diagnostics

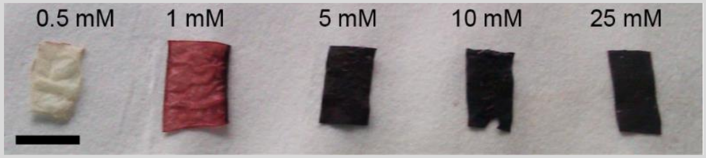

Computer analysis of SERS spectra

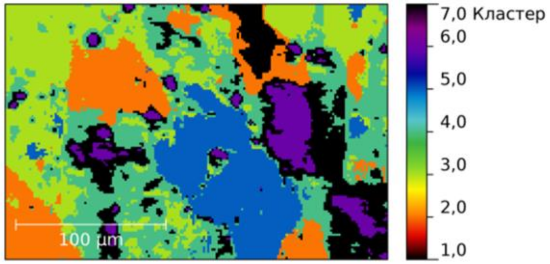

Imaging of cells and tissues

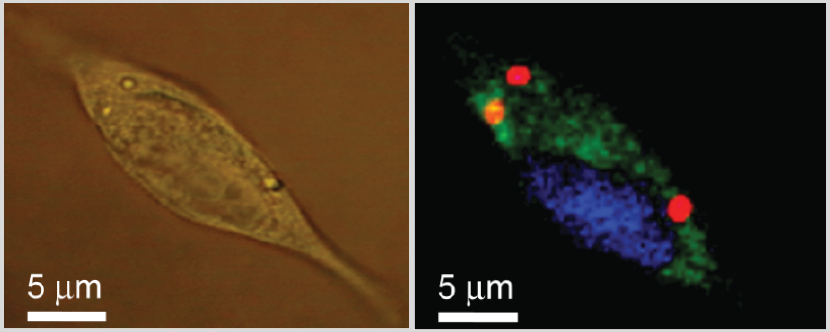

SERS of the D-Glucose in water

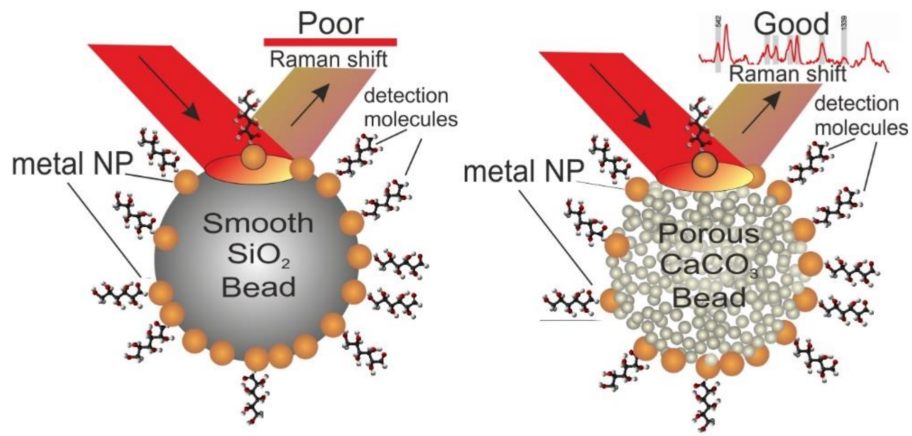

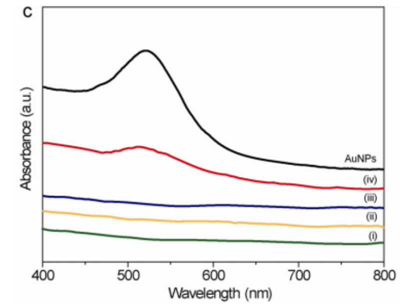

Glucose concentration in blood:

healthy ~ 70-150 mg/mL;

diabetics > 150 mg/mL.

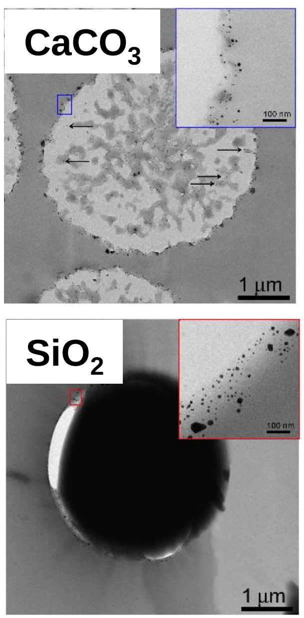

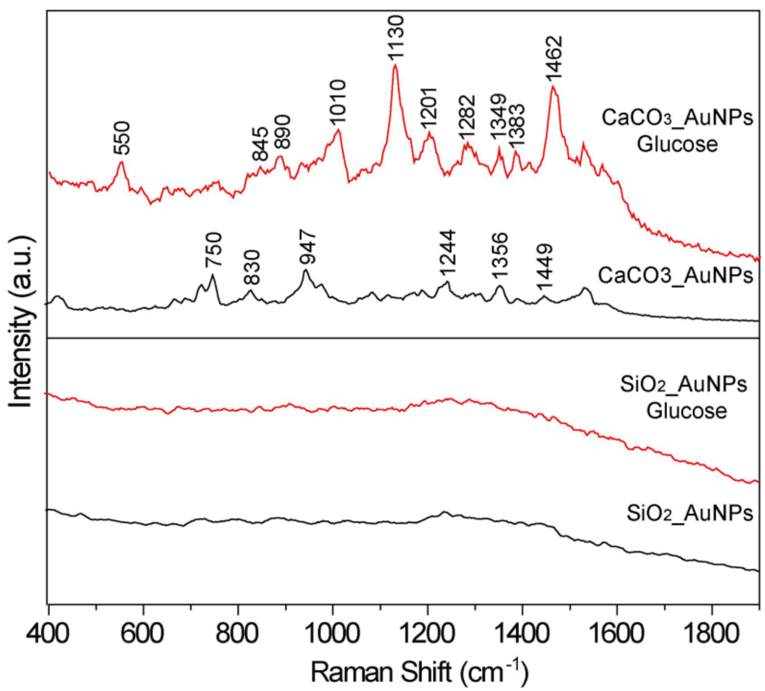

Glucose water solution 0.01 mg/mL

A.M. Yashchenok, D. Borisova, B.V. Parakhonskiy et. al, Ann. Phys. (Berlin) 2012, 524, 723.

SERS probes based on inorganic microparticles

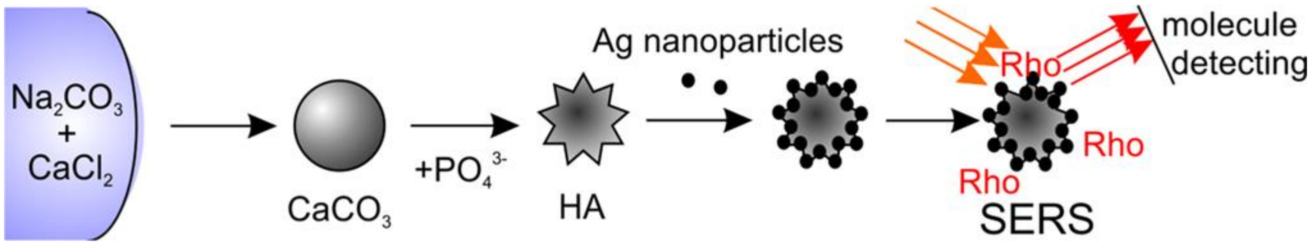

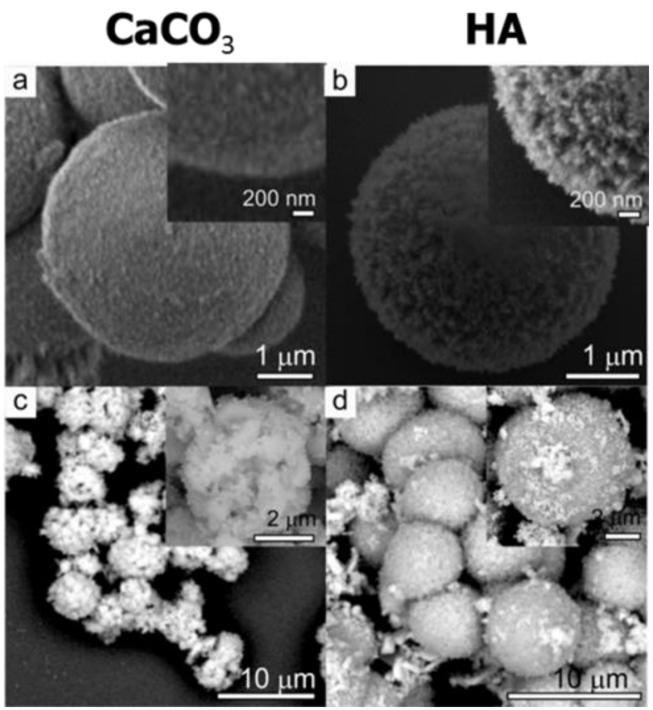

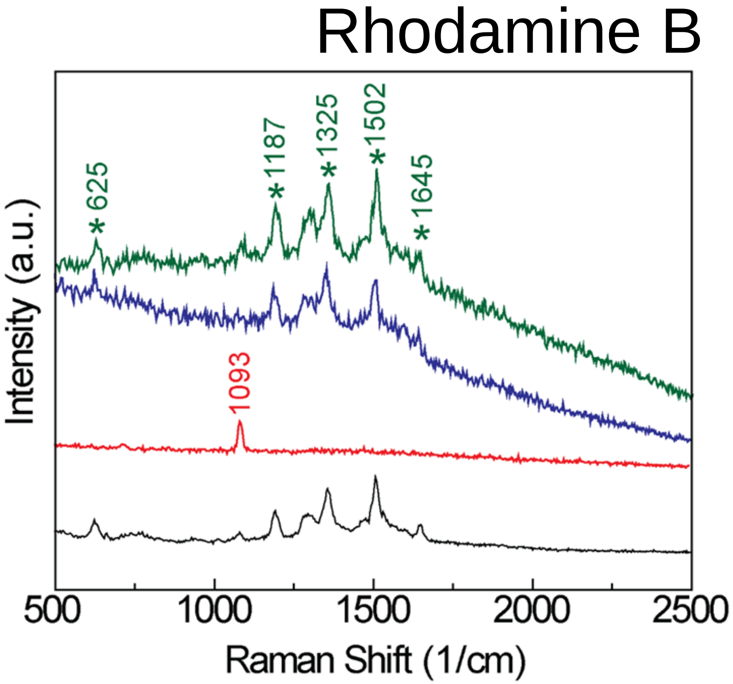

B.V. Parakhonskiy, Yu.I. Svenskaya, A.M. Yashchenok, et al., *Colloids and Surfaces B: Biointerfaces*, 2014, 118, 243.

SERS probe made of SWCNT/AuNPs

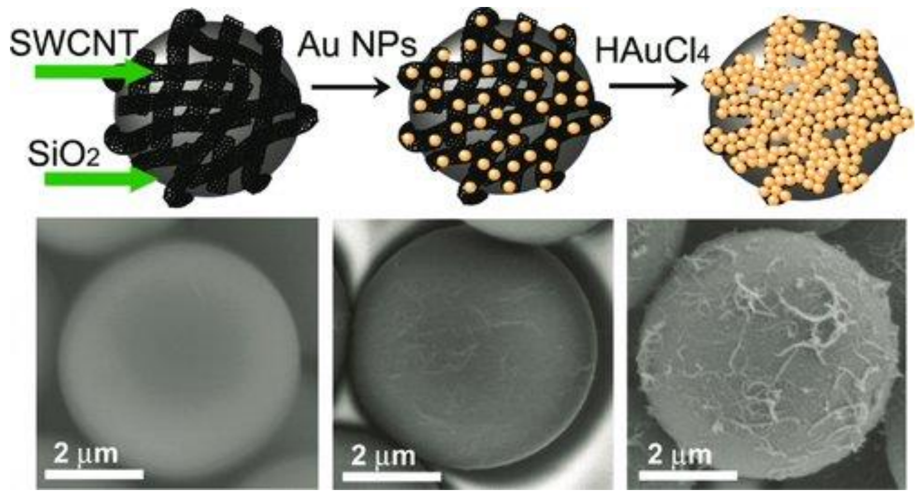

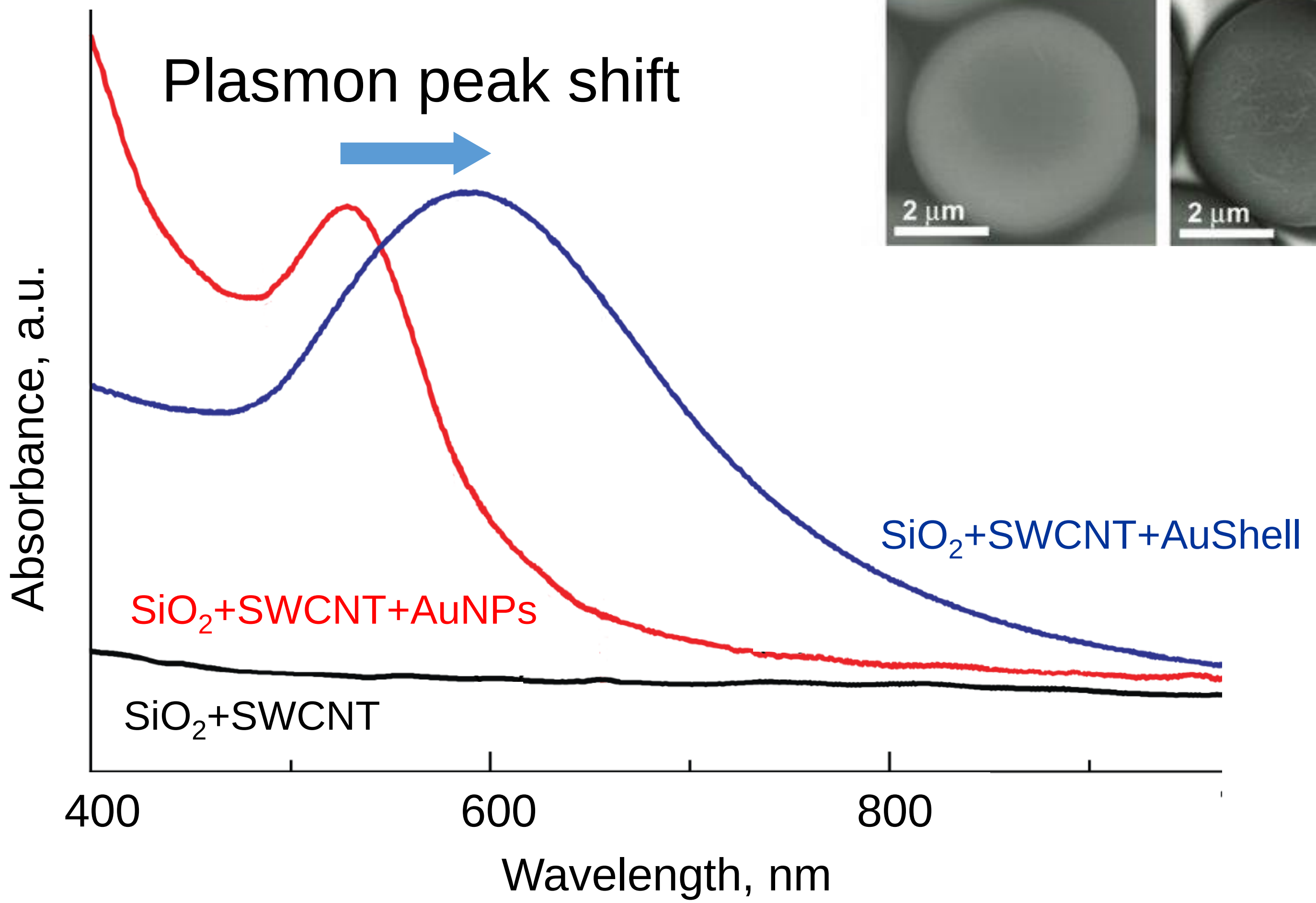

Yashchenok, A. Masic , D. Gorin et.al, Small 2013, 9, 351.

SWCNT G-band Enhancement

60-fold increase of G-band

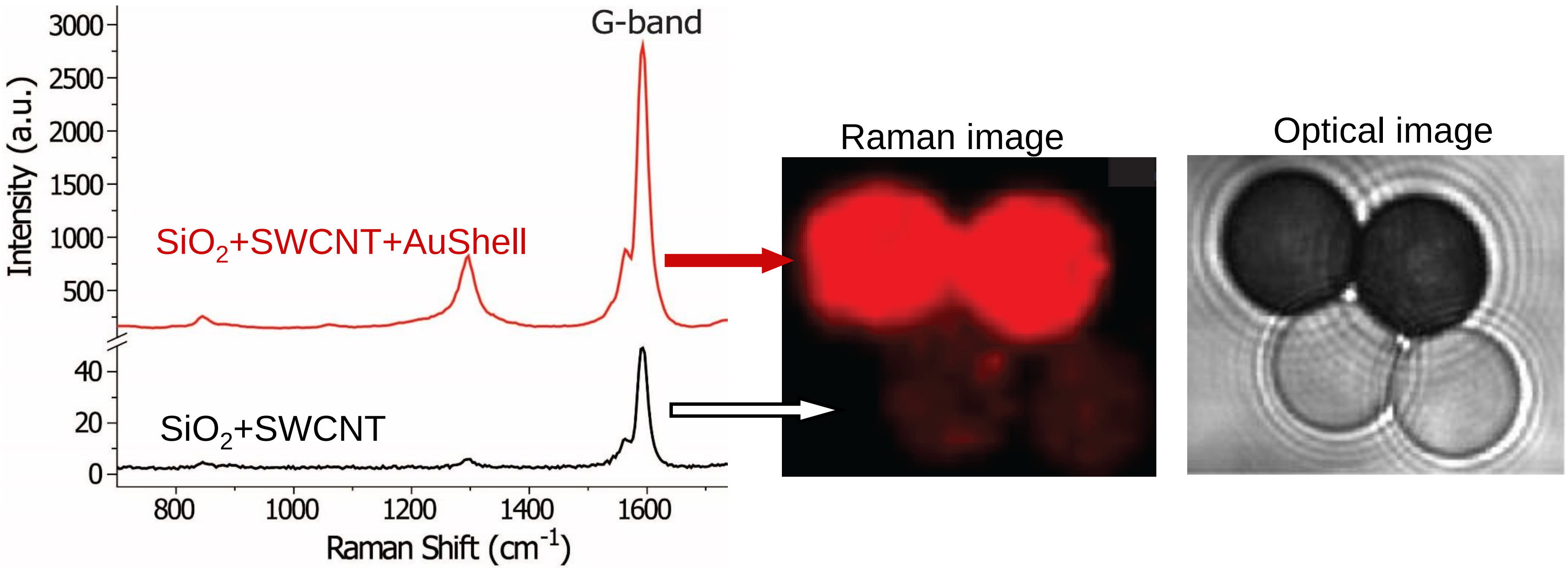

Laser power 0.1 mW, 785 nm

Yashchenok, A. Masic , D. Gorin et.al, Small 2013, 9, 351.

Intracellular SERS sensing

Signal to noise ration: non-resonant ~ 5; SERS ~100

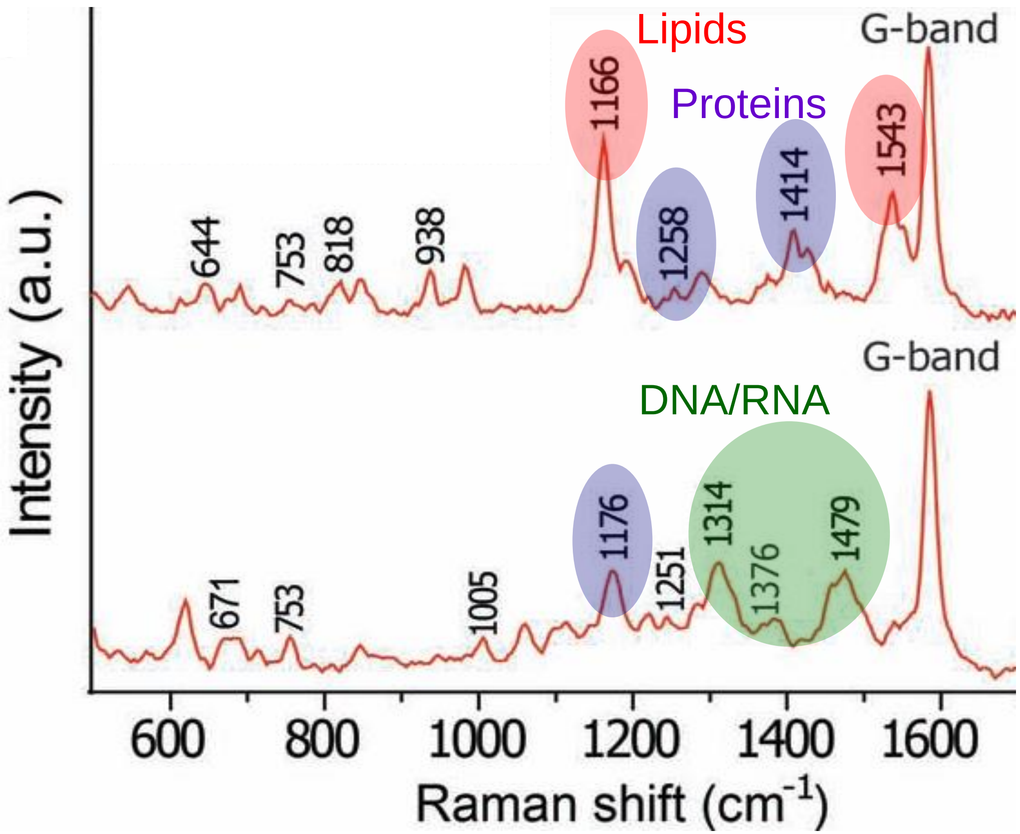

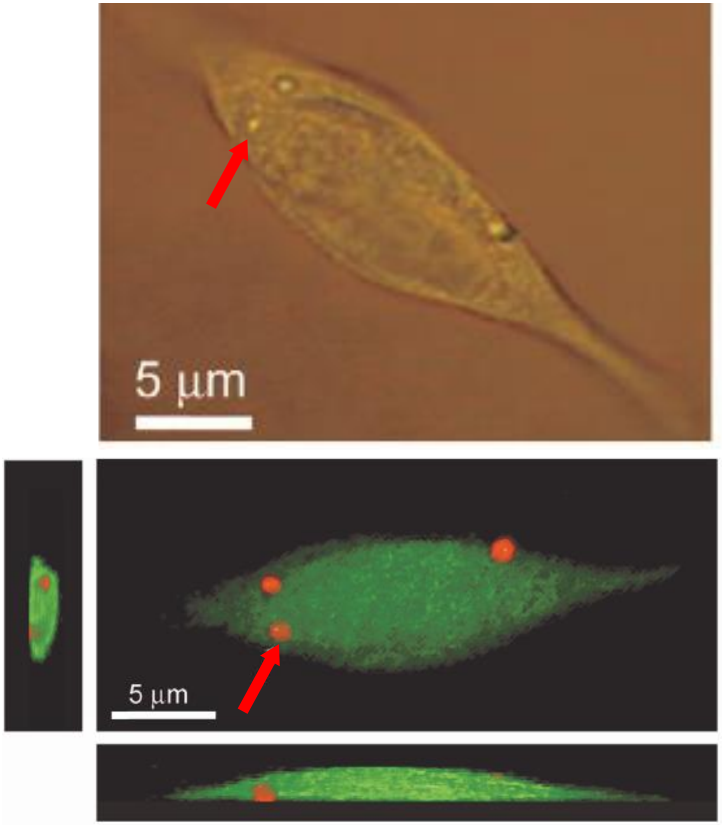

Yashchenok, A. Masic , D. Gorin et.al, Small 2013, 9, 351.

Laser-induced shift of the G-band

Air

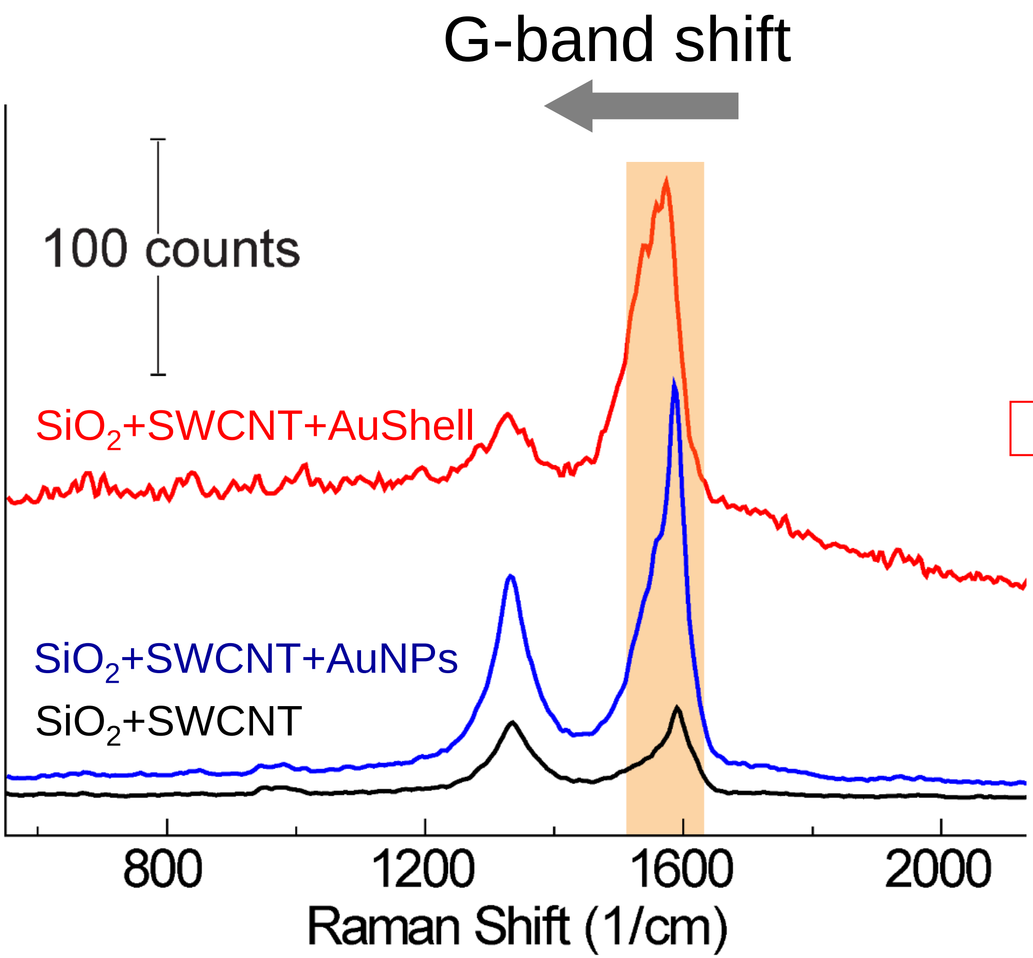

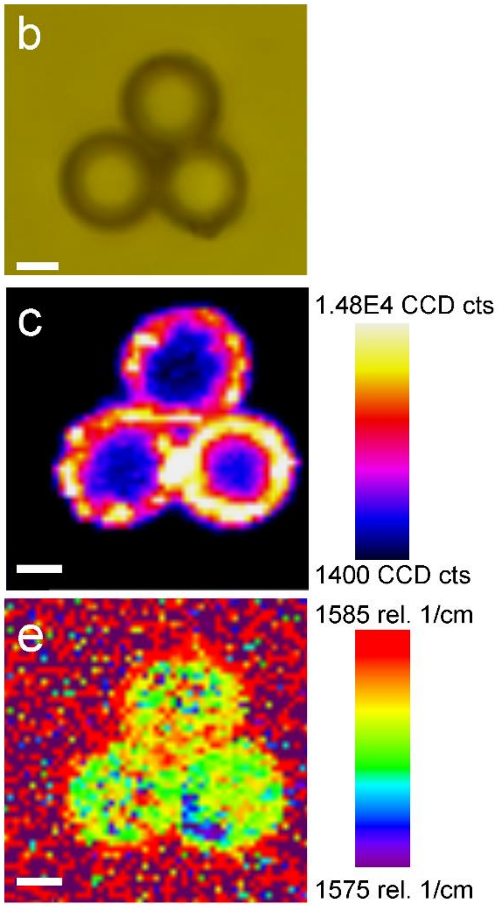

532 nm, power density ~ 12.7·10^4 W/cm^2

Yashchenok, A. Masic, D. Gorin, Small 2015, 11, 1320-1327.

The effective temperature assessment

SiO_2+SWCNT+AuShell

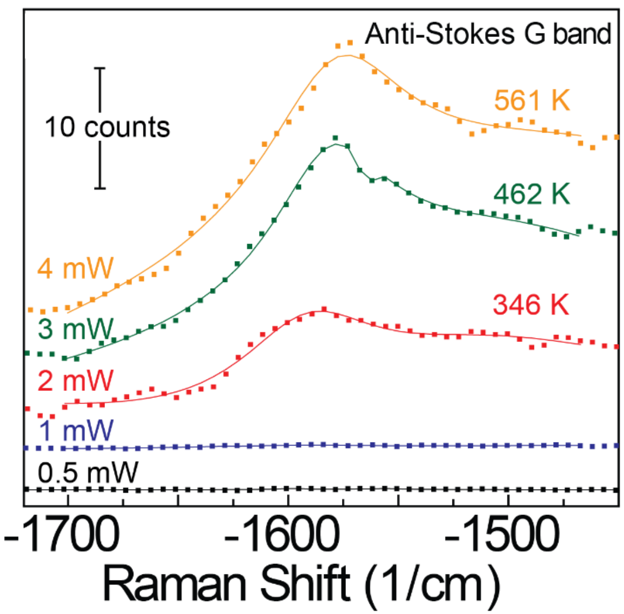

G-phonon

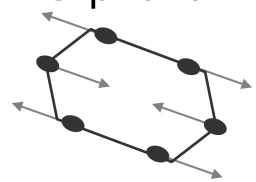

$$\frac{I_{AS}}{I_S} = \left(\frac{\nu_0 + \nu_G}{\nu_0 - \nu_G} \right)^4 \exp\left(-\frac{\hbar \nu_G}{k_B T_G} \right)$$

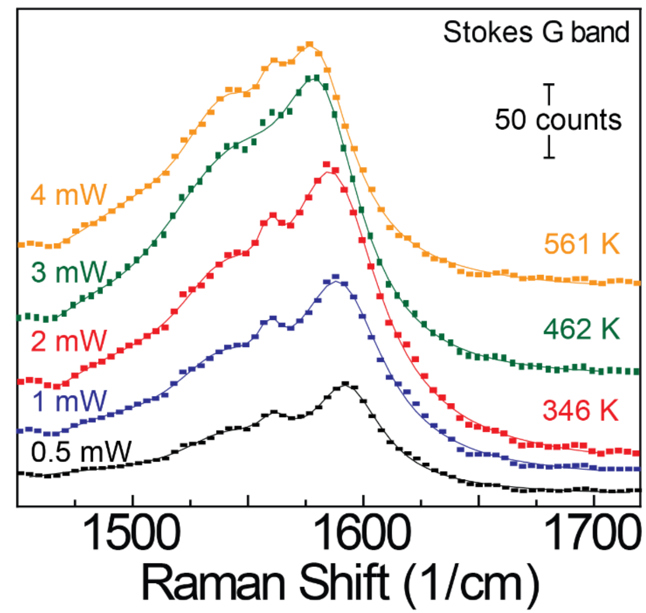

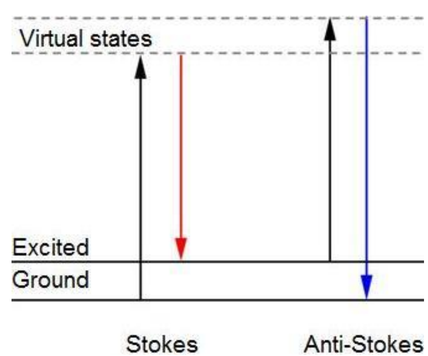

532 nm *Air*

Yashchenok, A. Masic, D. Gorin, Small 2015, 11, 1320-1327.

Heating and Cooling measurements

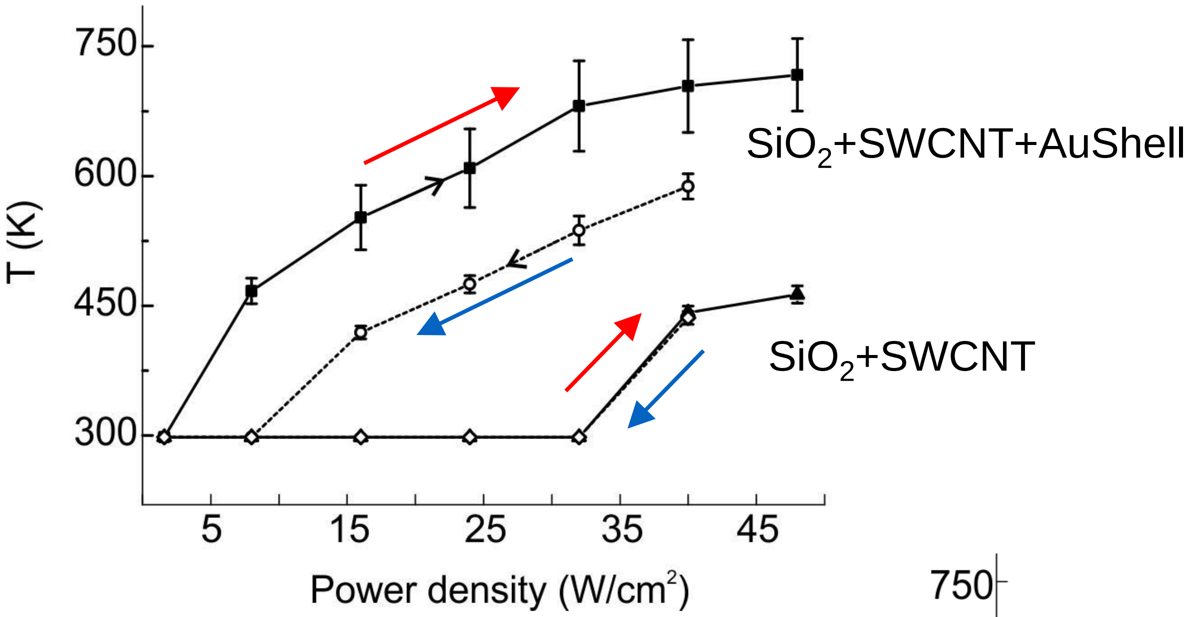

785 nm

Air

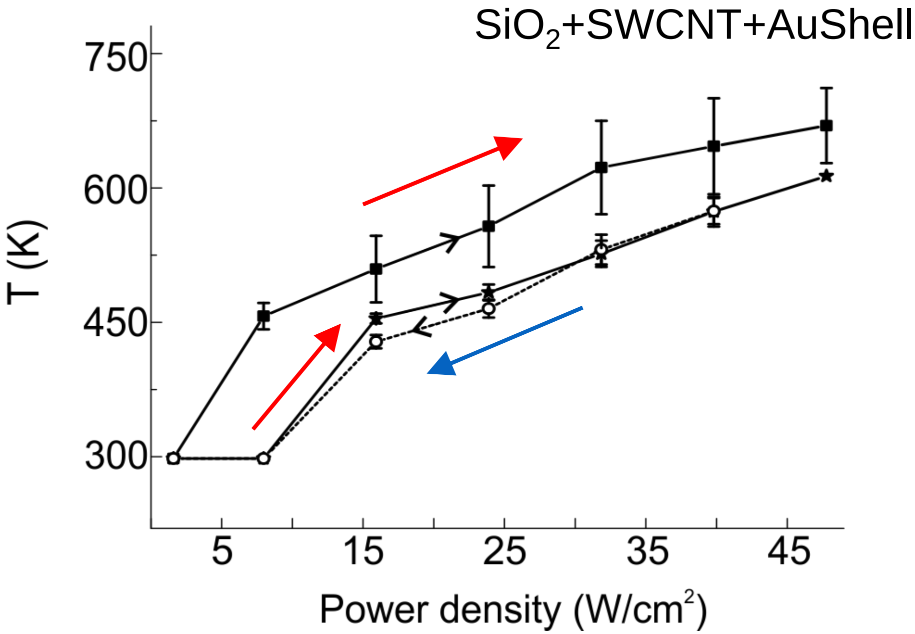

Yashchenok, A. Masic, D. Gorin, Small 2015, 11, 1320-1327.

Probe calibration

PS+SWCNT+AuShell

Air

4 mW, 532 nm

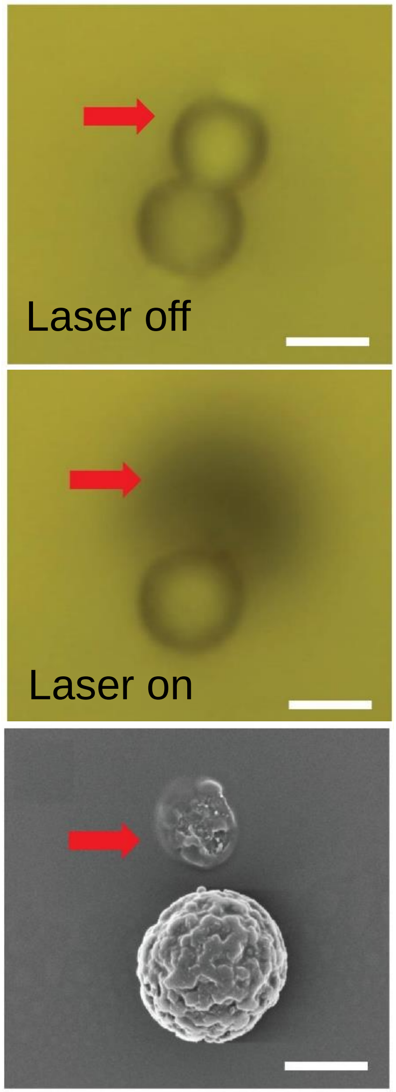

SiO_2+SWCNT+AuShell

Air

785 nm

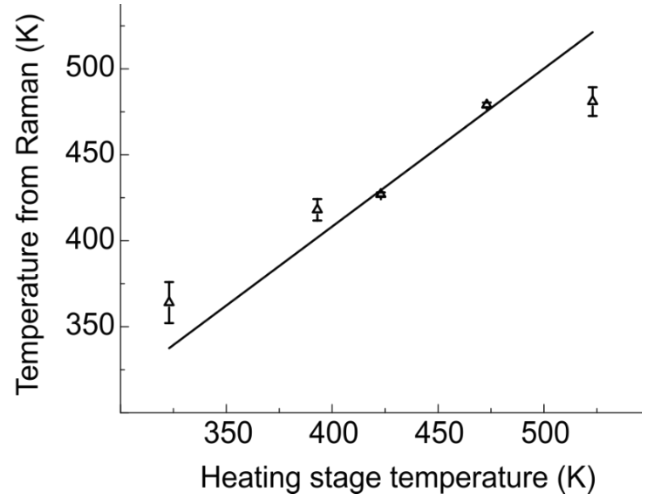

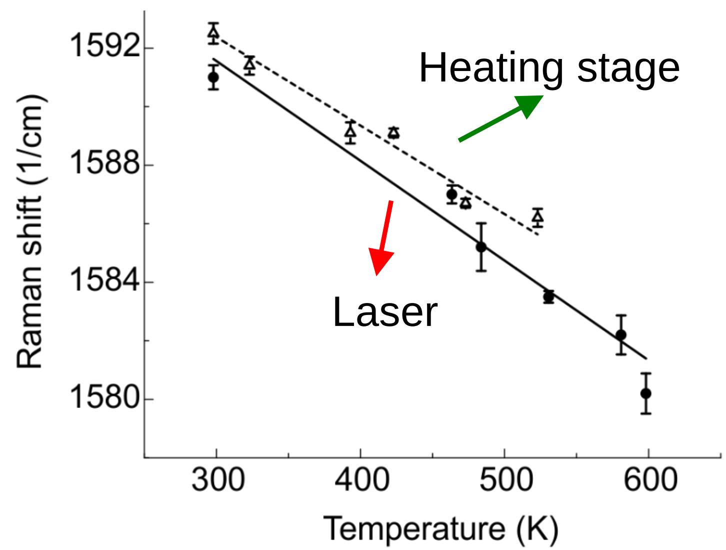

Yashchenok, A. Masic, D. Gorin, Small 2015, 11, 1320-1327.

Linkam THMS600 stage

SERS-based satellites

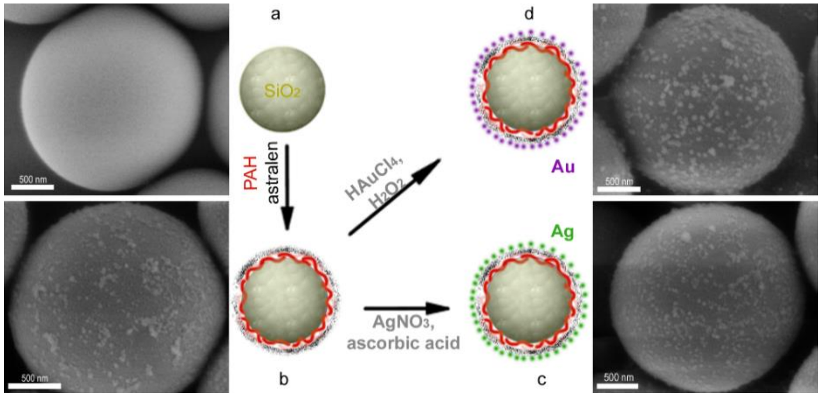

SiO_2/(PAH/Astralen)$_3$/Au

SiO_2/(PAH/Astralen)$_3$/Ag

L929 mouse fibroblast cell

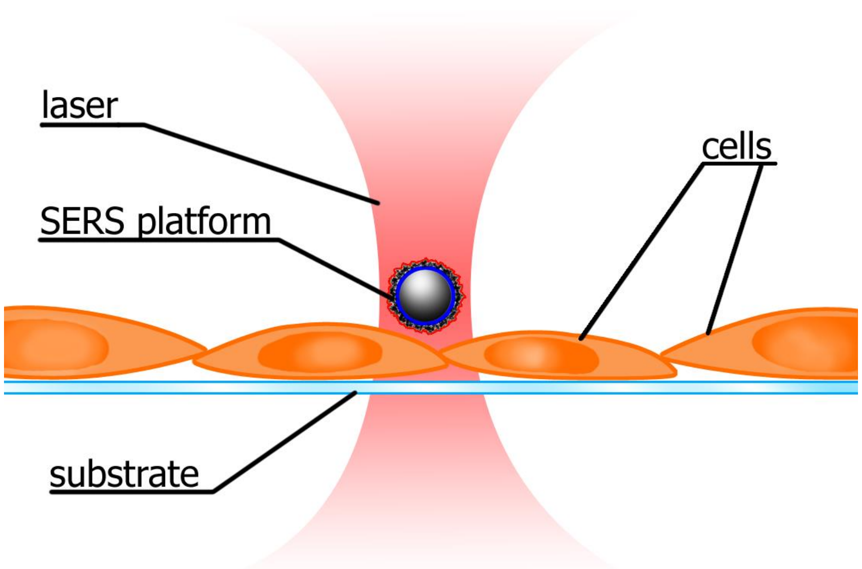

Laser tweezers at 976 nm

Analyst 2015 (accepted)

SERS-based satellites

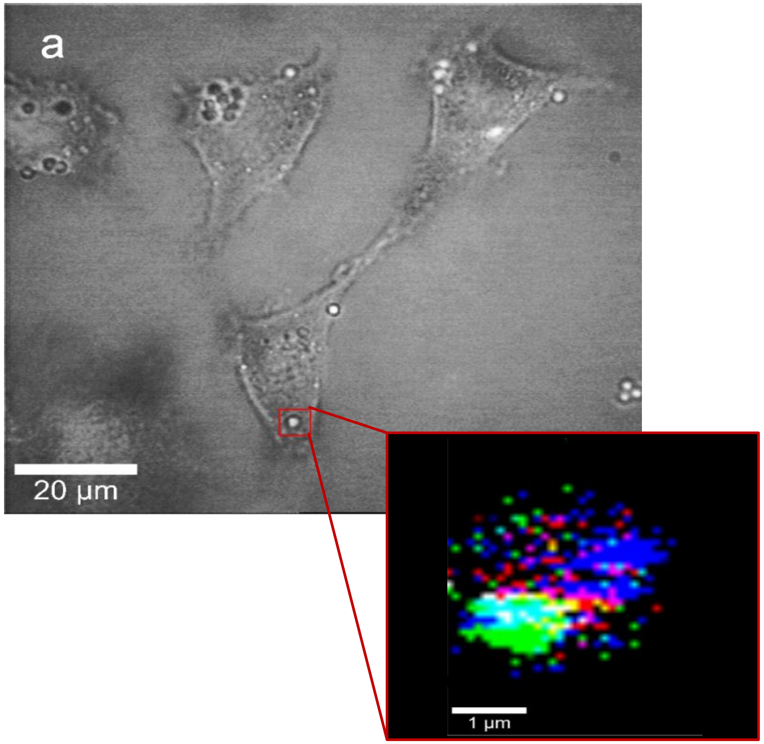

Raman imaging in the cell:

red – Astralen G-mode

blue – DNA bases

green – Lipids

785 nm, laser power of 0.2 µW

L929 mouse fibroblast cell

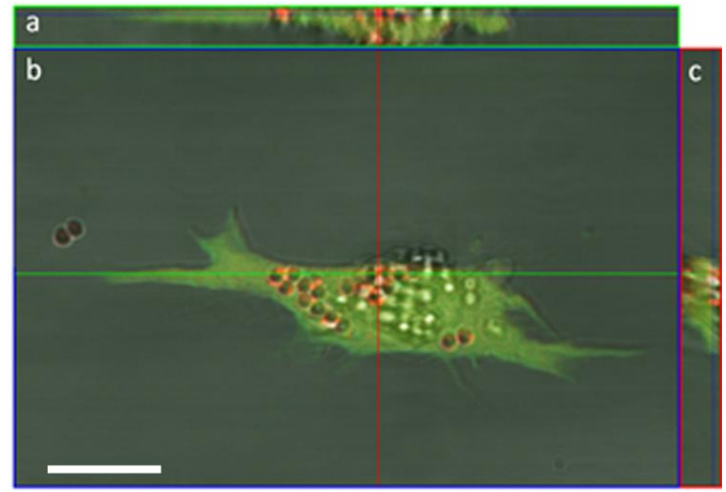

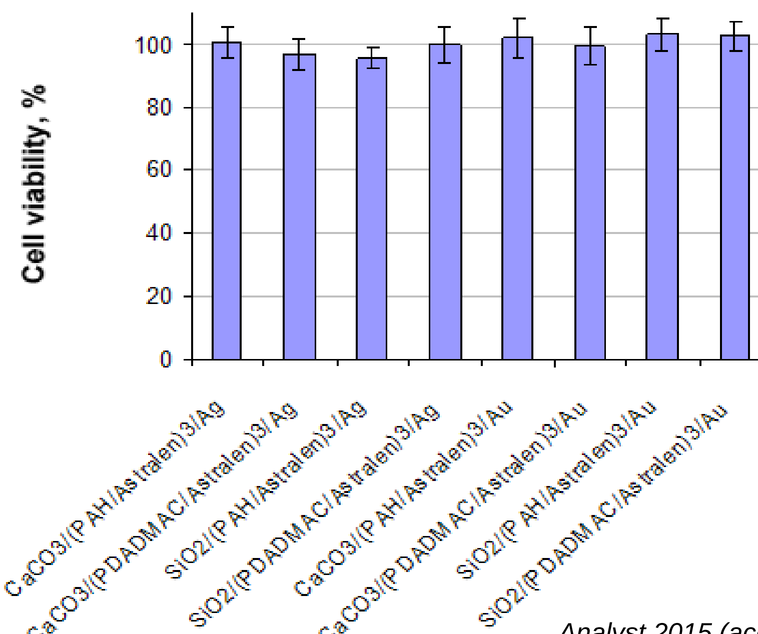

Analyst 2015 (accepted)

Intracellular SERS of Plasmonic Waveguides

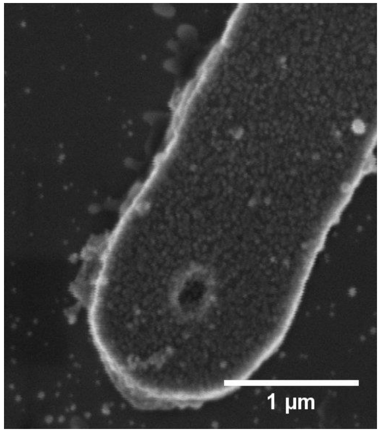

Human fibroblast cell

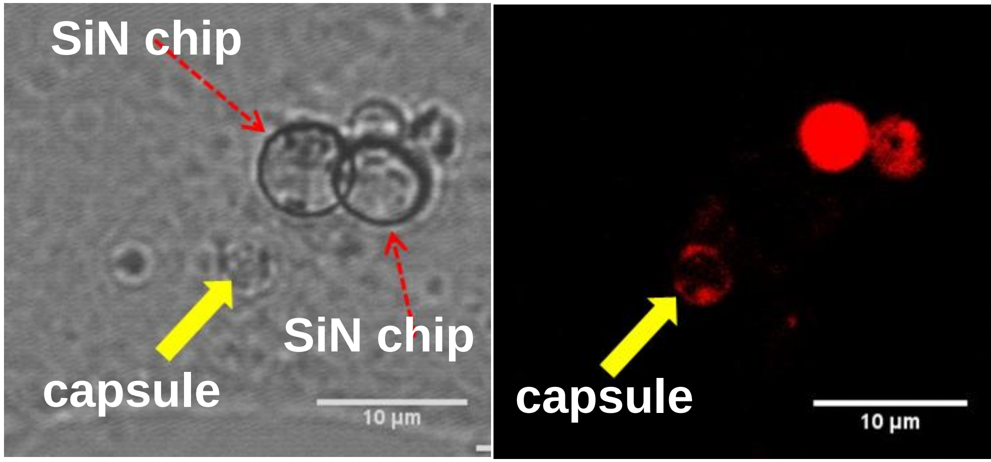

Gold-covered SiN particle d~200 nm.

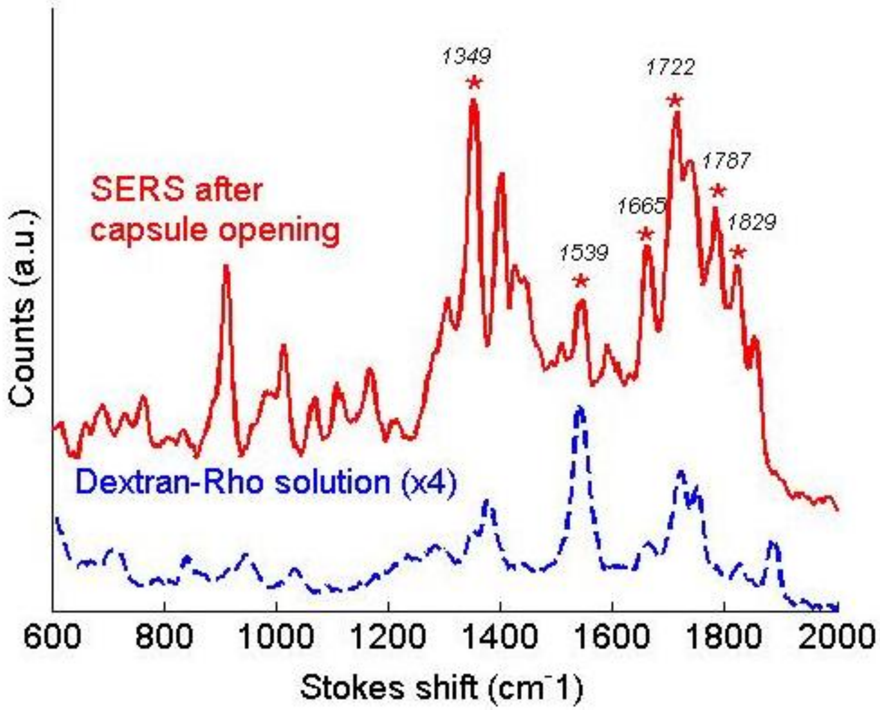

Nanoplasmonic Chitosan Nanofibers

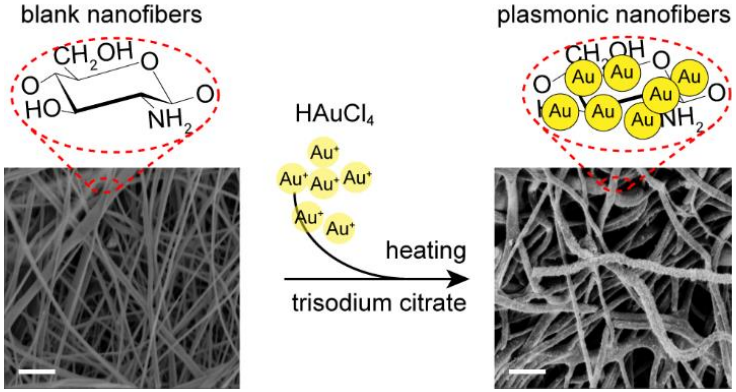

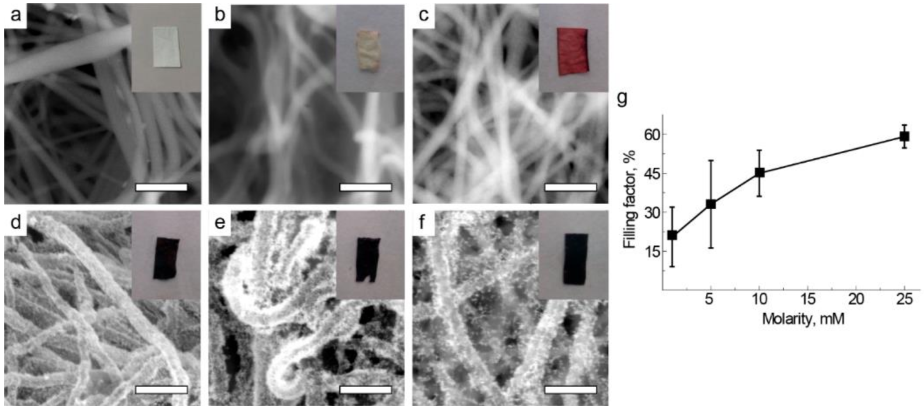

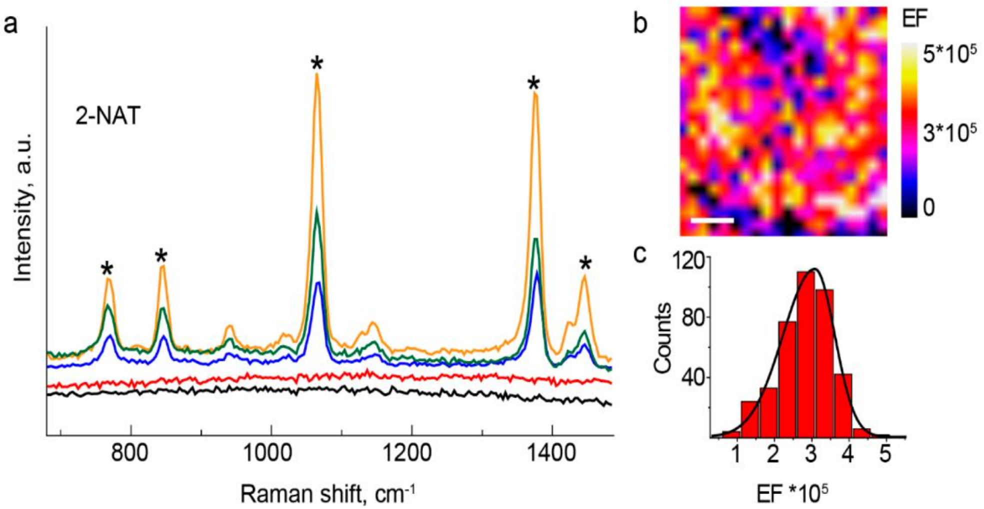

Immediate functionalization

Controlled distribution of AuNPs

EF of $2 \cdot 10^5$ for 86 % points

ACS Applied Mater and Inter, accepted

Nanoplasmonic Chitosan Nanofibers

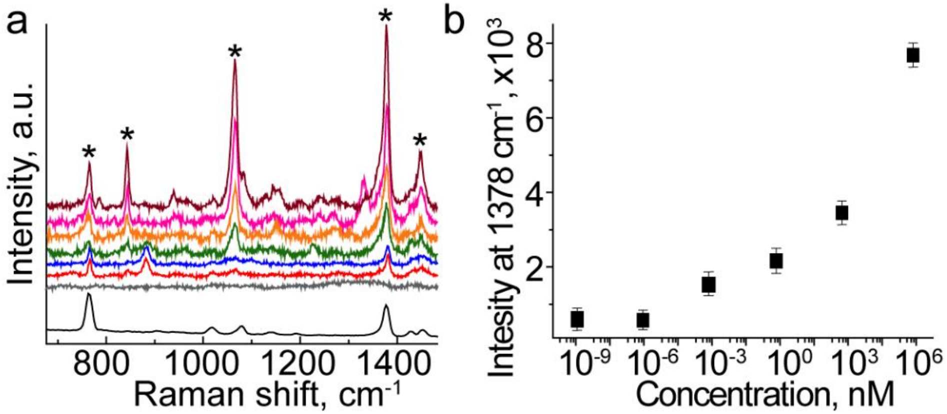

SERS detection of 2-naphthalenethiol with concentration less than 10^{-15} M

SERS detection of Rhodamine 6G and D-Glucose in micromolar range

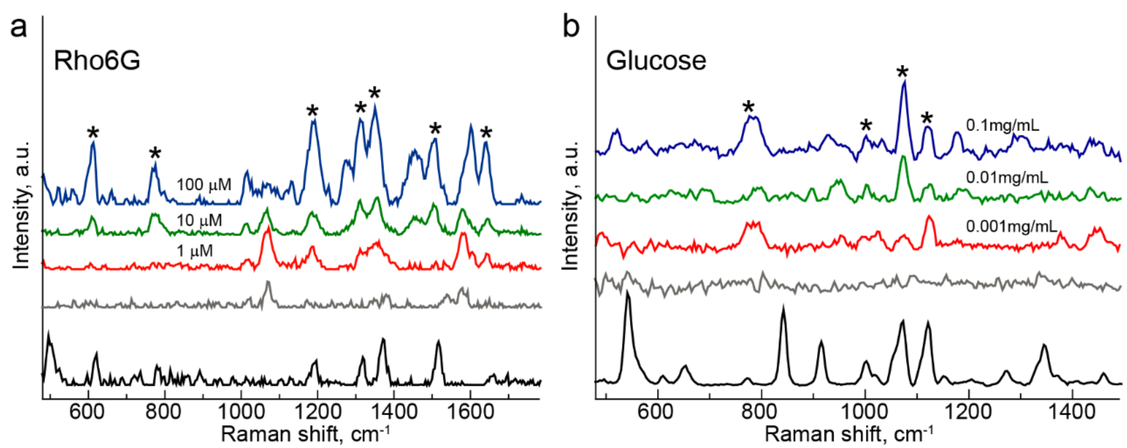

ACS Applied Mater and Inter, accepted

785 nm, 1% of laser power

Bifunctional Gold/Gelatin Hybrid Nanocomposites

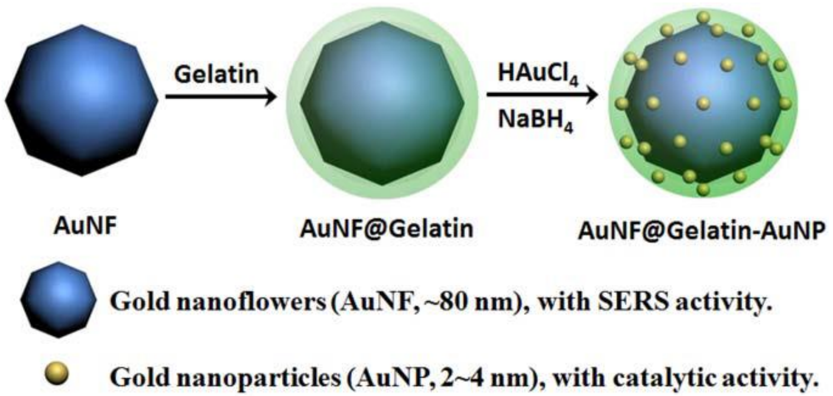

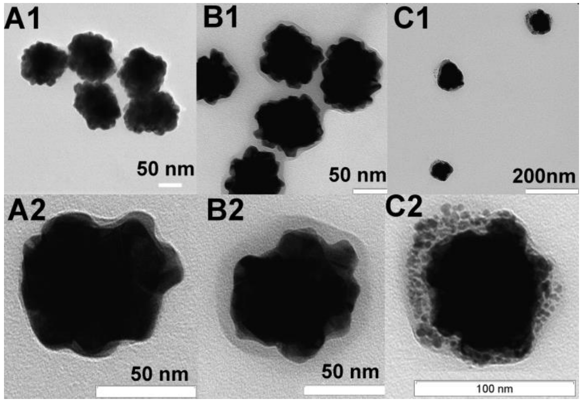

$NaBH_4$

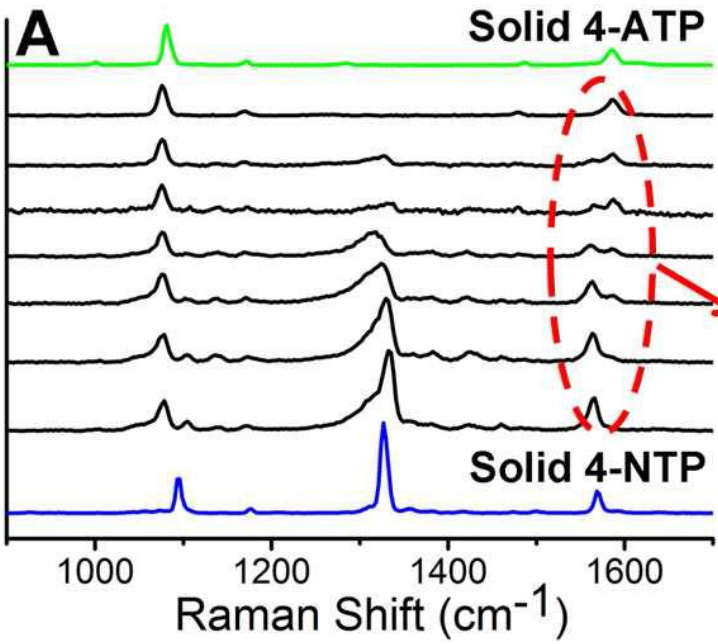

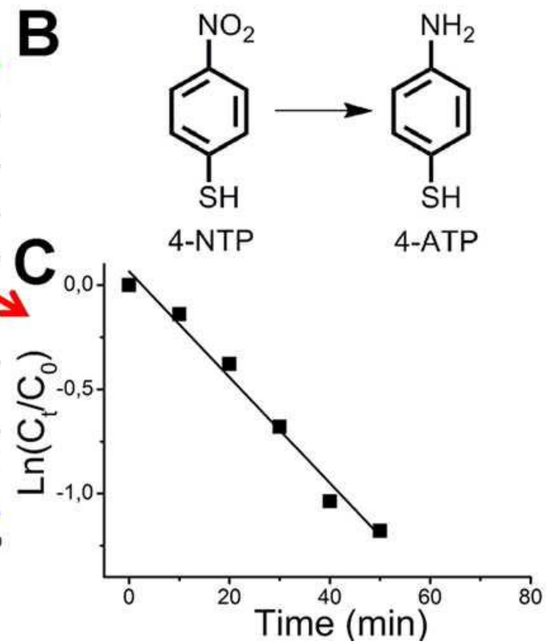

ACS Appl. Mater. Interfaces 2014, 6, 1999.

Photoacoustic Imaging

Optical Path

Pulsed Laser Illumination

Optical Absorption

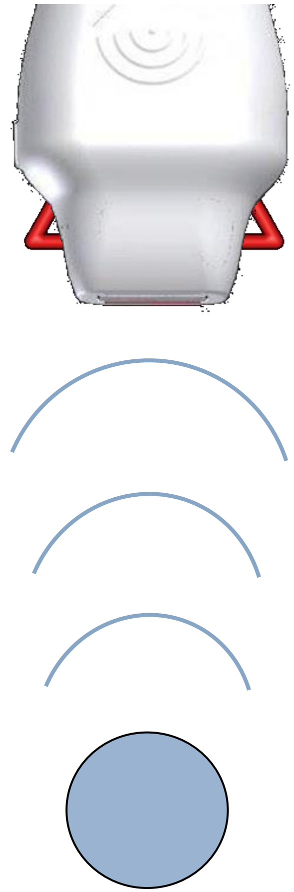

Sound Path

Acoustic Detection

Pressure Waves

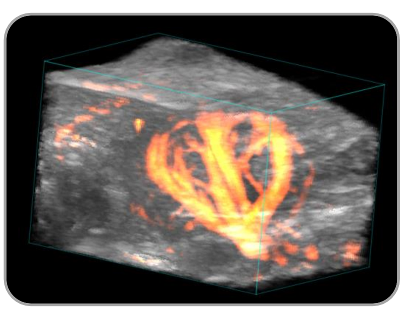

Thermal Elastic Expansion

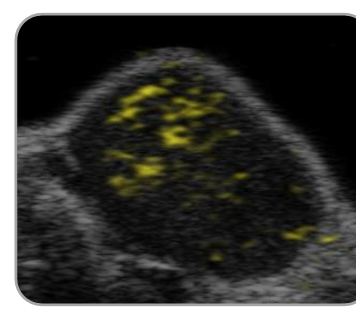

Visualization of microcapsules by photoacoustic

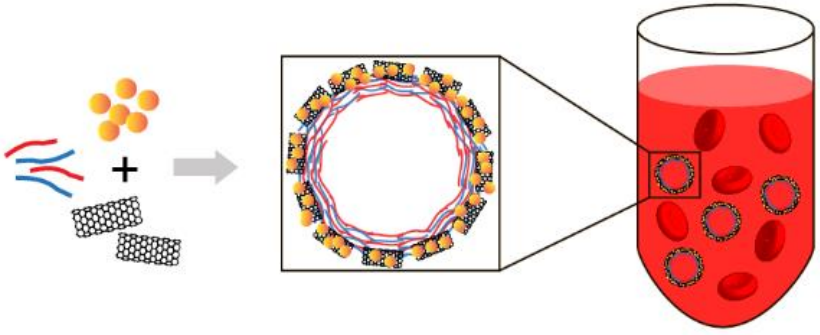

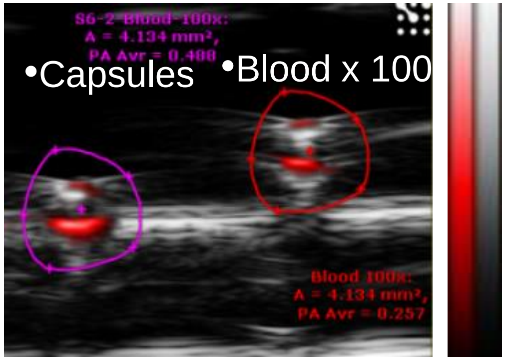

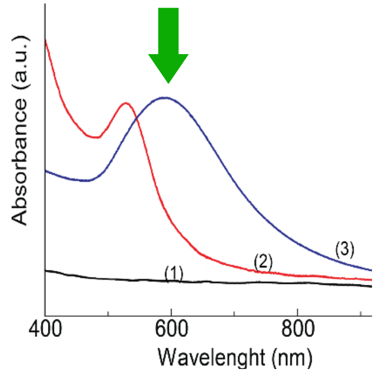

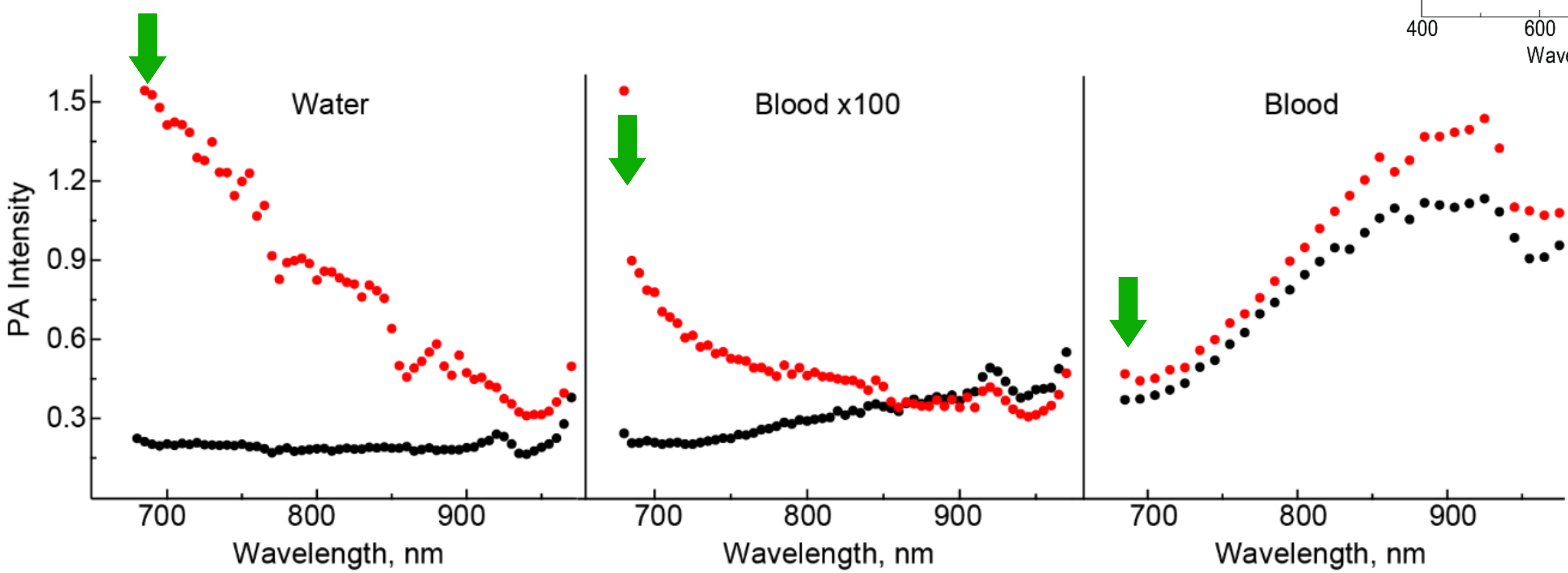

SERS of blood content

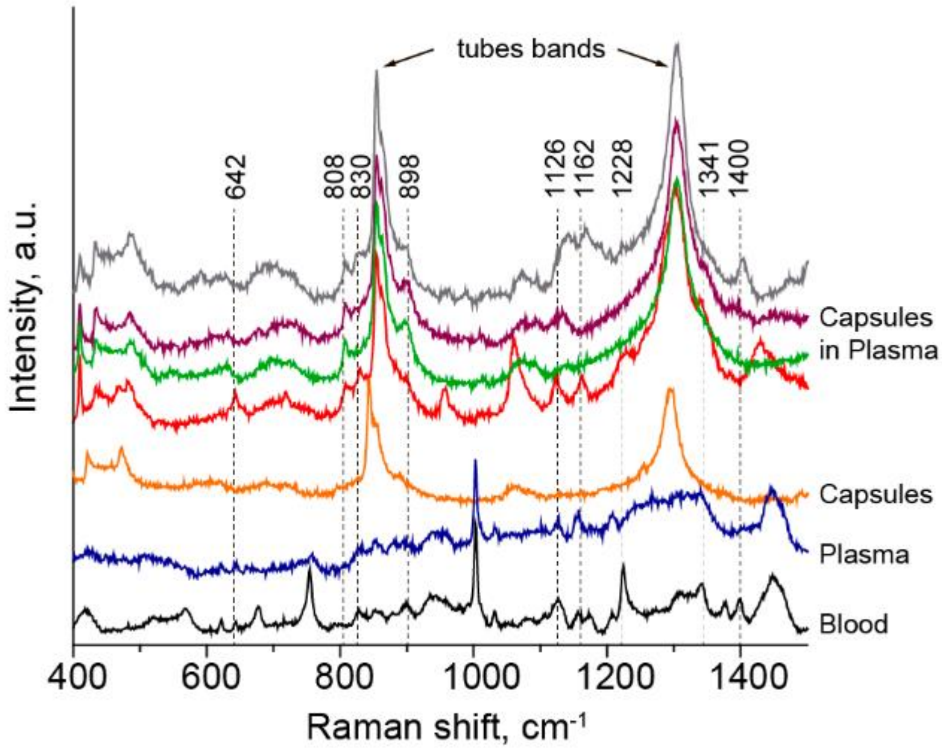

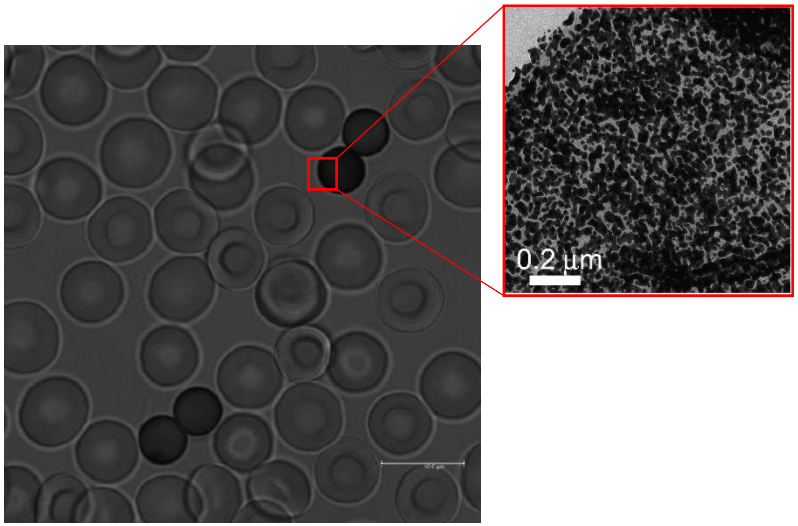

642 – C-C twisting (Tyrosine)
808 - C-C-O stretching (L-Serine)
830 – C-C stretching (Collagen)
898 – C-O-H bending (D-galactosamine)
1126 – D-mannos
1162 – Tyrosine
1228 – C-H methine in-plane bending
1341 – Adenin
1400 – C-H bending (Collagen)

Conclusions

- LbL and template-assited techniques are powerful tools for tuning optical properties of plasmonic microstructures
- SWCNT/AuNPs provides SERS enhancement at extremely low laser intensity
- The temperature is evaluated through the intensity ratio of the Anti-Stokes/Stokes
- Detection of biomolecules inside living cells with fast acquisition rates and at low laser power
- Monitoring the release of Dex-Rho from capsules inside living cells
- SERS detection of small molecules in micromolar range
- Photoacoustic imaging of capsules in blood

Collaborations and Acknowledgements

MPIKG Department of Interfaces
H. Möhwald, B.-E. Pinchasik, A. Heilig, R. Pitschke

MPIKG Department of Biomaterials
A. Masic, C. Pilz

Queen Mary University,School of Engineering and Material Sciences
G.B. Sukhorukov

Ghent University, Department of Information Technology, Department of Molecular Biotechnology
A. Skirtach, P.C. Wuytens

The Charité-Universitätsmedizin Berlin
H. Baemler, R. Georgieva

Michigan University, Department of Chemical Engineering
B.S. Shim, N.A. Kotov

Group Members

E. Prikhozdenko

D. Bratashov

I. Stecura

DAAD
Deutscher Akademischer Austausch Dienst
German Academic Exchange Service

Alexander von Humboldt
Stiftung/Foundation

The Organizing Committee

Thank you for your attention